ψ-Haar Wavelet Methods for Numerical Solution of Fractional Differential Equations

Amjid Ali

Department of Science and Engineering,
Graduate School of Science and Engineering,
Saga University, Japan

Candidate
Amjid Ali

Thesis
ψ-Haar Wavelet Methods for Numerical Solution of Fractional Differential Equations

Degree Awarded
Doctor of Philosophy in Science

Supervisor
Professor Teruya Minamoto

Affiliation
Department of Science and Engineering, Graduate School of Science and Engineering, Saga University, Japan

Dissertation Referees
Professor Teruya MINAMOTO (supervisor)
Professor Shin-ichi TADAKI
Associate Professor Takehiko KINOSHITA
Associate Professor Takuma KIMURA

Acknowledgments

My deepest gratitude goes to

- The Department of Science and Engineering, Graduate School of Science and Engineering, Saga University, Japan for providing a very exciting environment for a productive academic journey.
- My supervisor Professor Teruya Minamoto, whose supervision provided me great learning opportunities throughout my studies and for his encouragement, motivation, guidance and support towards accomplishment of this PhD study.
- Professor Toru Nakahara and his spouse for their guidance and financial support in difficult times during my PhD studies.
- Dr. Mujeeb ur Rehman and Dr. Umer saeed from NUST Pakistan for their excellent guidance and support during my stay in Pakistan.
- My lab mates: Dr. Ryuji Ohura, Dr. Hajime Omura for their cooperation.
- Saga University for providing me SIPOP (Strategic International Postgraduate Program) scholarship to support my Doctoral studies, Also many thanks go to staff of International Affair division for their support.
- My family for their support, patience, kindness and encouragement during my Ph.D. studies.

Amjid Ali

Declaration

I, AMJID ALI, proclaim that the work provided in this thesis titled, "ψ-Haar Wavelet Methods for Numerical investigation of Fractional Differential Equations" is my own. Here is what I confirm:

- This work was done mainly while as a candidate for a doctoral degree.
- It has been clearly stated if any part of this thesis has previously been submitted to this university for a degree or other qualification.
- I always give the source of quotes I have taken from other sources. It is entirely my own work, apart from such quotations.
- All sources of help have been acknowledged.
- I have specified exactly what others have done and what I myself have contributed.

AMJID ALI
February 2023

Abstract

Fractional differential equations are the best way to model many real-world physical phenomena. Apart from modelling, solution strategies and their implications are essential for determining critical points where a significant divergence or bifurcation begins. Therefore, high-precision solutions are always required. There are many different definitions of fractional derivatives in literature, one simple way to cope with this variation is to combine those concepts by considering fractional derivatives of a function with respect to another function ψ. Fractional differential equations with ψ-Caputo derivative provide more flexible models, in the sense that by a proper choice of function ψ, hidden features of the real-world phenomena could be extracted. The main objective of this study is to develop reliable and proficient numerical methods for solving linear and nonlinear Fractional Differential Equations(FDEs) involving ψ-Caputo fractional derivative. In this work, wavelets are the primary part for developing numerical schemes. We derived an operational matrix, called the ψ-Haar wavelet operational matrix, to find a numerical approximation of ψ- FDEs.

We extended the method to nonlinear ψ-FDEs by using ψ-Haar wavelet operational matrix method and quasilinearization technique. The quasilinearization techniques convert the fractional nonlinear differential equation to fractional discretized differential equation. ψ-Haar wavelet method is applied at each iteration of quasilinearization technique to get the approximate solution. The method is simple and good mathematical tool for finding solution of nonlinear ψ-FDEs. The operational matrix approach offers less computational complexity. The error analysis of the proposed method is discussed in-depth. Accuracy and efficiency of the method are verified through numerical examples.

Contents

List of Figures

List of Tables

Chapter 1

Introduction

Fractional calculus is as old as the classical calculus, and goes back to time when G. W. Leibniz and Newton invented differential calculus. In the 17^{th} century, G. W. Leibniz $(1646-1716)$ presented n^{th} order derivative symbol $\frac{d^n}{dx^n}$ for the first time. L'Hospital asked Leibniz how this operator works if number n is $1/2$. S. F. Lacroix was motivated by this question and formulated the formula for the arbitrary order derivative by use of Gamma function in his famous book published in 1819 [2]. The formula by Lacroix for α order derivative for x^m is $\frac{\Gamma(m+1)}{\Gamma(m-\alpha+1)}x^{m-\alpha}$. In [3], Joseph Liouville $(1809-1882)$ extended integer order derivative to fractional order α. This definition is considered to be the first formula for fractional derivative but that formula only applicable to the functions of the form $f(x)=\sum_{n=0}^{\infty}c_n e^{a_n x}$. Liouville formulated another formula to extend his first definition for fractional order derivative as $D^{\alpha}x^{-m}=(-1)^{\alpha}\frac{\Gamma(\alpha+m)}{\Gamma(m)}x^{-\alpha-m}$ for $m>0$. This definition only applicable to rational functions. Most scientist prefer Liouville's definition, however, Peacock supports the definition given by Lacroix. To avoid this conflict J. Fourier obtained the integral representation of function and its derivatives. Greer formulated fractional derivative for hyperbolic and trigonometric functions using first definition of Liouville. Various Mathematician including Hardy and Littlewood, Davis, Pitcher and Sewell, Debnath and Grum published a lot of research on fractional integral and derivative in 20^{th} century [4, 5]. Several books have been written on the philosophy and development of fractional calculus [6, 7, 8, 9].

In field of fractional calculus, Riemann-Liouville fractional derivative is note-worthy although it has specific drawbacks when trying to model physical problems that has inappropriate physical conditions. Caputo made a significant contribution by introducing the definition of fractional derivative that is suitable for modeling real world physical problems [10]. In addition, many other families of fractional operators have been introduced

until now. Due to many definitions of fractional operators, it was important to establish the generalized fractional operators for which the classical ones are particular cases. One of the extensions of Riemann-Liouville fractional operators are the so-called fractional operators of a function by another function (ψ-Riemann-Liouville fractional operators) which can be seen in [9, 11, 12]. In [1, 13] Almeida defined the Caputo version of fractional derivative of a function by another function, (ψ-Caputo fractional derivative) and studied its basic properties that plays a vital role in combining a large class of fractional operators. As an application of Caputo derivative of a function with respect to another function Almeida [1, 14] analyzed the world population growth modeled as FDE and showed that the choice of fractional derivative determines the accuracy of the model. Almeida et al. in [15] investigated existence and uniqueness results of nonlinear fractional differential equations involving a Caputo type derivative with respect to another function by means of fixed point theorems and developed Picard iteration method for solving the problem numerically. Almeida et al. in [16] provided a numerical method to solve fractional oscillation equations involving ψ-Caputo fractional derivative by introducing the ψ-fractional integral of ψ-shifted legendre polynomials. Almeida et al. has shown in [15] that the mathematical models with ψ-Caputo fractional derivatives are more flexible and ψ-Caputo fractional derivative has the potential to extract hidden aspects of real world phenomena.

A fractional differential equation (FDE) is a general form of ordinary differential equation(ODE). FDE's have many applications in different areas of science and engineering such as heat transfer in heterogeneous media [17], control theory, computational analysis [6, 9], fluid mechanics [18], dynamics of viscoelastic materials [19], biosciences [20], electromagnetism [21], continuum and statistical mechanics [22]. Most of the physical problems modeled as FDEs have no exact solution. Nevertheless in literature, there are some methods which are used for finding the exact solution of FDE's, like Transform methods, but these methods are limited to certain class of linear FDE's. Numerical approach is one of the best options to tackle different problems modeled as FDEs. Therefore, different numerical methods used for the approximate solutions to classical differential equations are extended to solve FDE's. Some of these methods include fractional difference method [23], differential transform method [24], Adomian decomposition method [25], and homotopy analysis method [26].

Wavelet methods are widely used in different numerical approximations being the most useful methods. Wavelets methods can be used for the numerical solutions of integral equations and numerical integration [27], ODEs [28], PDEs [29, 30] and FDEs [31]. For the detailed use and

application of the wavelets and various type of wavelets see Daubechies [32], Battle-Lemarie [33], B-spline [28], Chebyshev [34], Modified Chebyshev wavelets [35], a unified finite difference Chebyshev wavelet [36], Haar wavelets [37, 38, 39, 40], a unified approach for time fractional partial differential equations based on Haar wavelet, L1 discretization and Haar series [41], Legendre wavelets [42], sine-cosine wavelets [43] and Hermite wavelets [44].

Haar wavelet is also one of the best choices for solving FDEs and has been vastly used by many researchers. The simplicity of this method is one of its main advantages. Also it has better convergence in case of sharp transition of a function. Motivated by the above cited work on ψ-fractional derivative, we develop ψ-Haar wavelets Operational matrix method to solve linear and nonlinear fractional differential equations having ψ-Caputo fractional derivatives. For the convergence of the proposed technique we established an inequality in the context of error analysis. To check the efficiency of the suggested method we test some examples. The results of these examples are given in the graphical and tabular form. The thesis is organized as follows: In the first sections of Chapter 2, we introduced some special functions that were required for the development of our results. In the second section, the quasilinearization technique is discussed which is used for linearizing the nonlinear problems. In the third and fourth sections, some fundamental concepts, and definitions from fractional calculus and ψ-fractional calculus are provided. In section five, Haar wavelets and function approximation by Haar wavelets are given. Also, we constructed an operational matrix, called the ψ-Haar wavelet operational matrix. In the last section of chapter 2, the error analysis of the numerical scheme based on the ψ-Haar wavelets operational matrix is discussed in-depth. In chapter 3, we established a numerical scheme based on ψ-Haar wavelet operational matrices for solving linear and nonlinear initial value ψ-fractional differential equations. The quasilinearization technique is applied to convert the fractional nonlinear differential equation to a fractional to discretized differential equation. ψ-Haar wavelet method is applied at each iteration of the quasilinearization technique to get the approximate solution. We give some numerical examples utilizing the ψ-Haar wavelet operational matrix method to approximate the numerical solutions of linear and non-linear initial value fractional differential equations. The wavelet-based method reduces the problem to a system of algebraic equations. The numerical results obtained are compared with exact solutions by tabulating their absolute error and by comparing their respective graphs. It is worth mentioning that results obtained, agree well with exact solutions even for small number of collocation points. More accurate results are obtained by increasing the level of resolution J.

ψ-Haar wavelet technique has been extended, in Chapter 4, for linear and nonlinear fractional boundary value problems. Procedure of implementation of the method for general fractional differential equation has been introduced. This approach relies on the ψ-Haar wavelet operational integration matrices. The ψ-operational matrices are used to convert the ψ-Fractional Differential Equations to an algebraic system of equations. To handle the nonlinear case, we use quasilinearization technique to transform nonlinear ψ-fractional differential equation into linearized form and then ψ-Haar wavelets technique is applied in succession. The results obtained by the numerical scheme based on the ψ-Haar wavelet operational matrix method are compared with exact solutions. It has been observed that the results are in good agreement with the exact solution. The proposed method is a good and simple mathematical technique for numerically solving nonlinear ψ-fractional differential equations. The operational matrix method is computationally more efficient. Several linear and non-linear boundary value problems are discussed to demonstrate the applicability, efficiency, and simplicity of the method. The method is convenient for solving linear and nonlinear initial value problems as well as boundary value problems. It has been observed that the method gives more accurate results while increasing the level of resolution. In Chapter 5, a numerical method based on the two-dimensional ψ-Haar wavelets is discussed for numerical solutions of arbitrary order ψ-fractional partial differential equation. The method is applied to fractional initial and boundary value problems with constant coefficients and variable coefficients. We considered the time-fractional telegraph equation, linear fractional diffusion equation, and convection-diffusion equation with ψ-Caputo fractional derivative as test problems. A comparison of the approximate and exact solutions is carried out, results are given in the graphical and tabular form. It is observed that the solution becomes more accurate by increasing the level of resolution of the method. Operational matrices approach has been applied for the first time to solve ψ-fractional partial differential equations.

Chapter 2

Preliminaries

For the sake of convenience, we will review some necessary definitions and special functions. These are preliminaries in terms of fractional calculus which are going to aid in upcoming chapters.

2.1 Special Functions

In this part we review some basic special functions. These special functions are going to help in the upcoming chapters.

2.1.1 Euler's Gamma Function

Gamma function was introduced and defined by L. Euler in inspiration to sum up the factorial to whole number esteem. We observe that some well known scientific constants are happening in investigation of gamma function. It additionally appear in different fields such as geometric series, number theory and in definite integrals. The gamma function is defined in terms of definite integral as

$$\Gamma(x) = \int_0^\infty \xi^{x-1} e^{-\xi} d\xi, \qquad x > 0, \tag{2.1}$$

where the variable x is a dummy variable. We define some basic properties of Euler's gamma function

$$\Gamma(1) = 1$$

$$\Gamma(x+1) = x\Gamma(x).$$

An important relation between the gamma and beta function is defined as

$$\boldsymbol{\beta}(x_1, x_2) = \frac{\Gamma(x_1)\Gamma(x_2)}{\Gamma(x_1 + x_2)}, \qquad x_1, x_2 > 0.$$

The beta function can be defined as

$$\boldsymbol{\beta}(x_1, x_2) = \int_0^1 \xi^{x_1-1}(1-\xi)^{x_2-1} d\xi.$$

The beta function is utilized by Legendre, Whittaker and Watson in 1990 **is also called Eulerian integral of first kind.**

2.1.2 Mittag-Leffler Function

The earliest appearance of the Mittag-Leffler function dates back to 1903 **when Magnus Gosta Mittag-Leffler [45] presented the classical Mittag-Leffler function** $E_\alpha(z)$ **as a special function of the form**

$$E_\alpha(z) = \sum_{k=0}^{\infty} \frac{z^k}{\Gamma(\alpha k + 1)}, \ \alpha \in \mathbb{C}, \ \textbf{such that} \ \ \mathbb{R}e(\alpha) > 0. \tag{2.2}$$

After two years, Wiman [46] introduced the two-parameter Mittag-Leffler function $E_{\alpha,\beta}(z)$ **as**

$$E_{\alpha,\beta}(z) = \sum_{k=0}^{\infty} \frac{z^k}{\Gamma(\alpha k + \beta)}, \ \alpha \in \mathbb{C}, \ \textbf{such that} \ \ \mathbb{R}e(\alpha) > 0. \tag{2.3}$$

In 2007, **Shukla and Prajapati [47] presented a four-parameter Mittag-Leffler function** $E^{p,q}_{\alpha,\beta}(z)$ **defined as**

$$E^{p,q}_{\alpha,\beta}(z) = \sum_{k=0}^{\infty} \frac{(p)_{qk} z^k}{\Gamma(\alpha k + \beta) k!}, \qquad \alpha, \beta, p \in \mathbb{C} \ \textbf{and} \ q \in (0,1) \cap \mathbb{N}, \tag{2.4}$$

where $\mathbb{R}e(\alpha) > 0, \ \mathbb{R}e(\beta) > 0, \ \mathbb{R}e(p) > 0$ **and** $(p)_{qk} = \Gamma(p + qk)/\Gamma(p)$**.**

Lemma 2.1.1. *[10] For* $\theta \in \mathbb{R}, \ \gamma > 0$ *and* $\beta > 1$*, we have*

$${}_xD^\alpha_a (x-a)^{\beta-1} \mathbb{E}_{\gamma,\beta}[\theta(x-a)^\gamma] = (x-a)^{\beta-\alpha-1} \mathbb{E}_{\gamma,\beta-\alpha}[\theta(x-a)^\gamma], \tag{2.5}$$

and for $\beta = 1$ *and* $\alpha = \gamma$*, we have*

$${}_xD^\alpha_a \mathbb{E}_\alpha[\theta(x-a)^\alpha] = \theta \mathbb{E}_\alpha[\theta(x-a)^\alpha]. \tag{2.6}$$

2.2 Quasilinearization Technique

The technique named quasilinearization was presented by Kalaba and Bellman [48] as a generalization of a specific method (Newton-Raphson) [49] which assist in solving the nonlinear ordinary and partial differential equations. We explain the Quasilinearization technique to solve nonlinear fractional differential equations.

Consider the nonlinear fractional differential equation with boundary conditions

$$ {}_xD_a^\alpha y(x) = g(x, y(x)), \quad 1 < \alpha \leq 2, \quad x \in [0, 1], \tag{2.7} $$

subject to the boundary conditions $y(0) = \mu$ and $y(1) = \omega$. Suppose that the initial approximation of $y(x)$ is $y_0(x)$. Applying the Quasilinearization technique about y_0 to equation (2.7), we have

$$ {}_xD_a^\alpha y(x) = g(x, y_0(x)) + [y(x) - y_0(x)]g_{y_0}(x, y_0(x)), \tag{2.8} $$

which is a linear equation, solving (2.8) for $y(x)$ and assuming it $y_1(x)$ and expanding (2.7) with respect to $y_1(x)$, we have

$$ {}_xD_a^\alpha y(x) = g(x, u_1(x)) + [y(x) - y_1(x)]g_{y_1}(x, y_1(x)). \tag{2.9} $$

which is a third approximation. Assume that the iterative procedure converges, we continue the process till obtaining the desired accuracy. Therefore the recurrence relation can be written in the form

$$ {}_xD_a^\alpha y_{r+1}(x) = g(x, y_r(x)) + [y_{r+1}(x) - y_r(x)]g_{y_r}(x, y_r(x)), \tag{2.10} $$

with the conditions

$$ y_{r+1}(0) = \mu, \quad y_{r+1}(1) = \omega, $$

which is a sequence of linear fractional differential equations and the function $y_r(x)$ is known function which can be used to find the $y_{r+1}(x) \cong y(x)$.

2.3 Basic Definitions of Fractional Calculus

2.3.1 Riemann-Liouville Integral

Fractional integrals and derivatives are defined by the use of Cauchy's integral formula

$$ {}_x\mathcal{I}_a^n f(x) = \int_a^x \frac{(x-\xi)^{n-1} f(\xi)}{(n-1)!} d\xi. \tag{2.11} $$

where $n \in \mathbb{N}$, $f \in L_1[a, b]$ and $a, b \in \mathbb{R}$. By substituting gamma function for factorial in (2.11) leads to the definition of fractional integral.

Definition 2.3.1. *[10] The Riemann-Liouville fractional integral of order α is defined as, let $\alpha \in \mathbb{R}^+$ and the operator ${}_x\mathcal{I}_a^\alpha$ defined on $L_1[a,b]$ by*

$$({}_x\mathcal{I}_a^\alpha f)(x) = \frac{1}{\Gamma(\alpha)} \int_a^x (x-\xi)^{\alpha-1} f(\xi) d\xi, \tag{2.12}$$

is called Riemann-Liouville fractional integral operator or precisely R-L fractional integral operator.

For $\alpha = 0$, we have ${}_x\mathcal{I}_a^0 f = f$ which is the identity operator, if $\alpha \in \mathbb{N}$, then ${}_x\mathcal{I}_a^\alpha f$ coincides with the classical integral.

2.3.2 Riemann-Liouville Derivative

We discuss the concepts leading to definition of fractional differential operators. The fundamental theorem of integer order calculus gives ${}_xD_a^n {}_x\mathcal{I}_a^n f = f$, where $n \in \mathbb{N}$ denote the order of integral and differential operator. For $n_1, n_2 \in \mathbb{N}$ we can also write ${}_xD_a^{n_1-n_2} {}_x\mathcal{I}_a^{n_1-n_2} f = f$. Therefore we can write as,

$${}_xD_a^{n_2} f = {}_xD_a^{n_1} {}_x\mathcal{I}_a^{n_1-n_2} f. \tag{2.13}$$

If we replace n_2 by any $\alpha > 0$, relation (2.13) is valid for particular class of functions unless $n_1 - n_2 > 0$. This leads to the definition of Riemann-Liouville fractional differential operator.

Definition 2.3.2. *[10] For $\alpha \in \mathbb{R}^+$ The Riemann-Liouville fractional derivative can be defined as;*

$${}_x\hat{\mathbb{D}}_a^\alpha f(x) = \frac{1}{\Gamma(n-\alpha)} \Big(\frac{d}{dx}\Big)^n \int_a^x (x-\xi)^{n-\alpha-1} f(\xi) d\xi, \tag{2.14}$$

where $n-1 < \alpha \leq n$.

2.3.3 The Caputo fractional Differential Operator

The Rieman Liouville derivative assumed a noteworthy part in progression of hypothesis of fractional calculus. In theory of Riemann Liouville fractional derivative, we have seen that their are certain impediments of utilizing the Riemann Liouville differential operator for demonstrating this present reality wonders. It is to be noted that the Riemann Liouville derivative of a constant is not zero. To deal with these circumstances, in 1967 Caputo presented another definition of fractional derivative. Here we talk about the Caputo derivative, its properties and it's connection with the Riemann Liouville operators for integral and derivative [10].

Definition 2.3.3. *[10] Assume $\alpha \in \mathbb{R}^+ U \{0\}$ and $k = \lceil \alpha \rceil$, then*

$$
\begin{aligned}
{}^{*}D_a^{\alpha} f(t) &= I_a^{k-\alpha} D^k f(t) \\
&= \int_a^t \frac{(t-\eta)^{k-\alpha-1} D^k f(\eta)}{\Gamma(k-\alpha)} d\eta, \qquad a < t < b,
\end{aligned}
$$

the operator ${}^{*}D_a^{\alpha}$ is said to be α order Caputo differential operator.

Example 2.3.1. [10] Consider $\alpha,\ \beta \in \mathbb{R}^+$ and $f(x) = x^{\beta}$. The Caputo fractional derivative of $f(x)$ is given as

$$
{}_{x}D_0^{\alpha} f(x) = \frac{\Gamma(\beta+1)}{\Gamma(\beta-\alpha+1)} x^{\beta-\alpha}, \tag{2.15}
$$

provided that the right hand side of (2.15) is defined.

2.4 Basics of ψ-Fractional Calculus

This section reviews several concepts, definitions, and basic results from ψ-fractional calculus that are essential for subsequent advancements in thesis.

2.4.1 ψ-Fractional integral :

[50, 13] Let $h : \mathbf{J} \to \mathbb{R}$ be an integrable function, where $\mathbf{J} = [\delta_1, \delta_2]$ and $\alpha \in \mathbb{R}, n \in \mathbb{N}$ and $\psi(t) \in C^n(\mathbf{J})$ such that $\psi'(t) > 0\ \forall\ t \in \mathbf{J}$. The ψ-Riemann-Liouville fractional integral of order $\alpha > 0$ is defined as

$$
\mathcal{I}_{\delta_1}^{\alpha,\psi} h(t) = \frac{1}{\Gamma(\alpha)} \int_{\delta_1}^{t} \big(\psi(t) - \psi(s)\big)^{\alpha-1} \psi'(s) h(s) ds.
$$

Property 1:

$$
\mathcal{I}_{\delta_1}^{\eta,\psi} \mathcal{I}_{\delta_1}^{\zeta,\psi} h(t) = \mathcal{I}_{\delta_1}^{\eta+\zeta,\psi} h(t).
$$

2.4.2 ψ-Fractional Derivative :

[6, 1, 50, 13]
For $\alpha > 0$, $n - 1 < \alpha \leq n$, the ψ-Reimann-Liouville fractional derivative is given as

$$
D_{\delta_1}^{\alpha,\psi} h(t) = \left(\frac{1}{\psi'(t)} \frac{d}{dt} \right)^n \mathcal{I}_{\delta_1}^{n-\alpha,\psi} h(t).
$$

2.4.3 ψ-Caputo Fractional Derivative :[1]

For $n-1<\alpha\leq n$, ψ-Caputo fractional derivative of order α is defined as

$$ {}^{C}D_{\delta_1}^{\alpha,\psi}h(t)=\mathcal{I}_{\delta_1}^{n-\alpha,\psi}\left(\frac{1}{\psi'(t)}\frac{d}{dt}\right)^{n}h(t) $$

or

$$ {}^{C}D_{\delta_1}^{\alpha,\psi}h(t)=\mathcal{I}_{\delta_1}^{n-\alpha,\psi}h_{\psi}^{[n]}(t),\quad \textbf{where}\quad h_{\psi}^{[n]}(t)=\left(\frac{1}{\psi'(t)}\frac{d}{dt}\right)^{n}h(t) $$

ψ-Caputo fractional derivative can also be defined as

$$ {}^{C}D_{\delta_1}^{\alpha,\psi}h(t)=D_{\delta_1}^{\alpha,\psi}\big[h(t)-\sum_{\kappa=0}^{n-1}\frac{h_{\psi}^{[\kappa]}(\delta_1)}{\kappa!}(\psi(t)-\psi(\delta_1))^{\kappa}\big] $$

where $n=\lceil\alpha\rceil$ for $\alpha\notin\mathbb{N}$ and $n=\alpha$ for $\alpha\in\mathbb{N}$.

Property 2: [1, 13]

If $h(t)=\big(\psi(t)-\psi(\delta_1)\big)^{\zeta}$ where $\zeta>n$ and $\alpha>0$ then

$$ {}^{c}D_{\delta_1}^{\alpha,\psi}h(t)=\frac{\Gamma(\zeta+1)}{\Gamma(\zeta-\alpha+1)}\Big(\psi(t)-\psi(\delta_1)\Big)^{\zeta-\alpha}. $$

Property 3:[1, 13]

$$ {}^{c}D_{\delta_1}^{\alpha,\psi}\mathcal{I}_{\delta_1}^{\alpha,\psi}h(t)=h(t). $$

Proof By definition

$$ {}^{c}D_{\delta_1}^{\alpha,\psi}\mathcal{I}_{\delta_1}^{\alpha,\psi}h(t)=D_{\delta_1}^{\alpha,\psi}\big[\mathcal{I}_{\delta_1}^{\alpha,\psi}h(t)-\sum_{\kappa=0}^{n-1}\frac{[\mathcal{I}_{\delta_1}^{\alpha,\psi}h(t)]_{\psi}^{[\kappa]}(\delta_1)}{\kappa!}(\psi(t)-\psi(\delta_1))^{\kappa}\big]. \tag{2.16} $$

Note that

$$
\begin{aligned}
[\mathcal{I}_{\delta_1}^{\alpha,\psi}h]_{\psi}^{[\kappa]}(t) &= \left(\frac{1}{\psi'(t)}\frac{d}{dt}\right)^{\kappa}\mathcal{I}_{\delta_1}^{\alpha,\psi}h(t)\\
&= \left(\frac{1}{\psi'(t)}\frac{d}{dt}\right)^{\kappa-1}\frac{1}{\psi'(t)}\frac{d}{dt}\int_{\delta_1}^{t}\frac{\big(\psi(t)-\psi(s)\big)^{\alpha-1}}{\Gamma(\alpha)}\psi'(s)h(s)ds\\
&= \left(\frac{1}{\psi'(t)}\frac{d}{dt}\right)^{\kappa-1}\frac{1}{\psi'(t)}\int_{\delta_1}^{t}\frac{(\alpha-1)\big(\psi(t)-\psi(s)\big)^{\alpha-2}}{\Gamma(\alpha)}\psi'(t)\psi'(s)h(s)ds\\
&= \left(\frac{1}{\psi'(t)}\frac{d}{dt}\right)^{\kappa-1}\int_{\delta_1}^{t}\frac{\big(\psi(t)-\psi(s)\big)^{\alpha-2}}{\Gamma(\alpha-1)}\psi'(s)h(s)ds\\
&= \left(\frac{1}{\psi'(t)}\frac{d}{dt}\right)^{\kappa-1}\mathcal{I}_{\delta_1}^{\alpha-1,\psi}h(t)
\end{aligned}
$$

$$
[\mathcal{I}_{\delta_1}^{\alpha,\psi}h]_{\psi}^{[\kappa]}(t) = \left(\frac{1}{\psi'(t)}\frac{d}{dt}\right)^{\kappa-1}\mathcal{I}_{\delta_1}^{\alpha-1,\psi}h(t).
$$

Repeating the process κ-times we are at

$$
[\mathcal{I}_{\delta_1}^{\alpha,\psi}h]_{\psi}^{[\kappa]}(t) = \mathcal{I}_{\delta_1}^{\alpha-\kappa,\psi}h(t) \tag{2.17}
$$

using equation (2.17) **in equation** (2.16)**, we have**

$$
{}^{c}D_{\delta_1}^{\alpha,\psi}\mathcal{I}_{\delta_1}^{\alpha,\psi}h(t) = D_{\delta_1}^{\alpha,\psi}\big[\mathcal{I}_{\delta_1}^{\alpha,\psi}h(t) - \sum_{\kappa=0}^{n-1}\frac{\mathcal{I}_{\delta_1}^{\alpha-\kappa,\psi}h(\delta_1)}{\kappa!}(\psi(t)-\psi(\delta_1))^{\kappa}\big]. \tag{2.18}
$$

Now we show that $\mathcal{I}_{\delta_1}^{\alpha-\kappa,\psi}h(\delta_1) = 0$, that is $\lim_{t\to a}\mathcal{I}_{\delta_1}^{\alpha-\kappa,\psi}h(t) = 0$.

$$
\begin{aligned}
\|\ \mathcal{I}_{\delta_1}^{\alpha,\psi}h(t)\| &= \|\frac{1}{\Gamma(\alpha)}\int_{\delta_1}^{t}\big(\psi(t)-\psi(s)\big)^{\alpha-1}\psi'(s)h(s)ds\|\\
&\leq \frac{1}{\Gamma(\alpha)}\int_{\delta_1}^{t}\|\big(\psi(t)-\psi(s)\big)^{\alpha-1}\psi'(s)h(s)ds\|\\
&\leq \frac{\|h\|}{\Gamma(\alpha)}\int_{\delta_1}^{t}\big(\psi(t)-\psi(s)\big)^{\alpha-1}\psi'(s)h(s)ds\\
&\leq \|h\|\frac{\big(\psi(t)-\psi(\delta_1)\big)^{\alpha}}{\Gamma(\alpha+1)}.
\end{aligned}
$$

Hence $\mathcal{I}_{\delta_1}^{\alpha,\psi}h(t) \to 0$ as $t \to \delta_1$. From equation (2.18)**, we have**

$$\begin{aligned}
{}^{c}D_{\delta_1}^{\alpha,\psi}\mathcal{I}_{\delta_1}^{\alpha,\psi}h(t) &= D_{\delta_1}^{\alpha,\psi}\mathcal{I}_{\delta_1}^{\alpha,\psi}h(t) \\
&= \left(\frac{1}{\psi'(t)}\frac{d}{dt}\right)^{n}\mathcal{I}_{\delta_1}^{n-\alpha,\psi}\mathcal{I}_{\delta_1}^{\alpha,\psi}h(t) \\
&= \left(\frac{1}{\psi'(t)}\frac{d}{dt}\right)^{n}\mathcal{I}_{\delta_1}^{n-\alpha+\alpha,\psi}h(t) \\
&= \left(\frac{1}{\psi'(t)}\frac{d}{dt}\right)^{n}\mathcal{I}_{\delta_1}^{n,\psi}h(t).
\end{aligned}$$

Consequently, ${}^{c}D_{\delta_1}^{\alpha,\psi}\mathcal{I}_{\delta_1}^{\alpha,\psi}h(t) = h(t)$. As we know that

$$\begin{aligned}
\frac{1}{\psi'(t)}\frac{d}{dt}\mathcal{I}_{\delta_1}^{1,\psi}h(t) &= \frac{1}{\psi'(t)}\frac{d}{dt}\int_{\delta_1}^{t}\big(\psi(t)-\psi(s)\big)^{1-1}\psi'(s)h(s)ds \\
&= \frac{1}{\psi'(t)}\psi'(t)h(t), \ \textbf{(Leibniz rule)} \\
&= h(t),
\end{aligned}$$

by repeating above process n-times we have

$$\Big(\frac{1}{\psi'(t)}\frac{d}{dt}\Big)^{n}\mathcal{I}_{\delta_1}^{n,\psi}h(t) = h(t).$$

Lemma 2.4.1.

$$\mathcal{I}_{\delta_1}^{n,\psi}h_{\psi}^{[n]}(t) = h(t) - \sum_{\kappa=0}^{n-1}\frac{h_{\psi}^{[n]}(\delta_1)}{\kappa!}\big(\psi(t)-\psi(\delta_1)\big)^{\kappa}.$$

Proof. For $n = 1$,

$$\begin{aligned}
\mathcal{I}_{\delta_1}^{1,\psi}h_{\psi}^{[1]}(t) &= \int_{\delta_1}^{t}\frac{\big(\psi(t)-\psi(s)\big)^{1-1}}{\Gamma(1)}\psi'(s)\frac{1}{\psi'(s)}\frac{d}{ds}h(s)ds \\
&= \int_{\delta_1}^{t}\frac{d}{ds}h(s)ds \\
&= h(t) - h(\delta_1).
\end{aligned} \tag{2.19}$$

For $n = 2$,

$$\begin{aligned}
\mathcal{I}_{\delta_1}^{2,\psi} h_{\psi}^{[2]}(t) &= \mathcal{I}_{\delta_1}^{1,\psi} \mathcal{I}_{\delta_1}^{1,\psi} \big[h_{\psi}^{[1]}\big]_{\psi}^{1}(t) \\
&= \mathcal{I}_{\delta_1}^{1,\psi} \big[h_{\psi}^{[1]} - h_{\psi}^{[1]}\big] \quad \text{by} \quad (2.19) \\
&= \mathcal{I}_{\delta_1}^{1,\psi} h_{\psi}^{[1]}(t) - \mathcal{I}_{\delta_1}^{1,\psi} h_{\psi}^{[1]}(\delta_1) \\
&= h(t) - h(\delta_1) - h_{\psi}^{[1]}(\delta_1) \int_{\delta_1}^{t} (\psi(t) - \psi(\delta_1))^{1-1} \psi'(s) ds \\
&= h(t) - h(\delta_1) - h_{\psi}^{[1]}(\delta_1)(\psi(t) - \psi(\delta_1)).
\end{aligned} \tag{2.20}$$

By repeating above process n-times, we get

$$\mathcal{I}_{\delta_1}^{n,\psi} h_{\psi}^{[n]}(t) = h(t) - \sum_{\kappa=0}^{n-1} \frac{h_{\psi}^{[\kappa]}(\delta_1)}{\kappa!} \big(\psi(t) - \psi(\delta_1)\big)^{\kappa}.$$

The proof of lemma 2.4.1 is completed. □

Lemma 2.4.2.

$$\mathcal{I}_{\delta_1}^{\alpha,\psi} \ {}^{C}D_{\delta_1}^{\alpha,\psi} h(t) = h(t) - \sum_{\kappa=0}^{n-1} \frac{h_{\psi}^{[\kappa]}(\delta_1)}{\kappa!} (\psi(t) - \psi(\delta_1))^{\kappa}.$$

Proof. Since

$${}^{C}D_{\delta_1}^{\alpha,\psi} h(t) = \mathcal{I}_{\delta_1}^{n-\alpha,\psi} h_{\psi}^{[n]}(t),$$

thus

$$\begin{aligned}
\mathcal{I}_{\delta_1}^{\alpha,\psi} {}^{C}D_{\delta_1}^{\alpha,\psi} h(t) &= \mathcal{I}_{\delta_1}^{\alpha,\psi} \mathcal{I}_{\delta_1}^{n-\alpha,\psi} h_{\psi}^{[n]}(t) \\
&= \mathcal{I}_{\delta_1}^{\alpha+n-\alpha,\psi} h_{\psi}^{[n]}(t) \\
&= \mathcal{I}_{\delta_1}^{n,\psi} h_{\psi}^{[n]}(t)
\end{aligned}$$

$$\mathcal{I}_{\delta_1}^{\alpha,\psi} {}^{C}D_{\delta_1}^{\alpha,\psi} h(t) = h(t) - \sum_{\kappa=0}^{n-1} \frac{h_{\psi}^{[\kappa]}(\delta_1)}{\kappa!} \big(\psi(t) - \psi(\delta_1)\big)^{\kappa}.$$

□

2.5 Haar wavelets and function approximation

Haar wavelets were first introduced by the Hungarian Mathematician Alfred Haar in 1990. Haar wavelets are the simplest wavelets among various wavelets families that has a compact support. Wavelets with compact

support are proven to be a good tool for numerical approximation of the functions. The Haar wavelets family consist of step functions defined on real line, which means that they are not continuous and hence at the points of discontinuity the derivatives do not exist. To overcome this drawback, the higher order derivatives appearing in the differential equations are first expanded into Haar series [38]. The lower order derivatives and the solutions can then be obtained quite easily by using Haar operational matrix of integration [51, 52, 53].
All functions in the Haar wavelet family defined on the interval $[a, b]$ are given by :

$$h_i(x) = \begin{cases} 1, & \textbf{if } \ x \in [\xi_1(i), \xi_2(i)); \\ -1, & \textbf{if } \ x \in [\xi_2(i), \xi_3(i)); \\ 0, & \textbf{otherwise}, \end{cases} \tag{2.21}$$

where $\xi_1(i) = a+(b-a)\frac{k}{m}$, $\xi_2(i) = a+(b-a)\frac{2k+1}{2m}$, $\xi_3(i) = a+(b-a)\frac{k+1}{m}$ **and** $m = 2^j$, **where** $j = 0, 1, 2, 3, ..., J$ **and** $k = 0, 1, 2, 3, ..., m-1$**. Here, the parameters** j **and** k **represent dilation and translation of the wavelet, respectively, while** J **represents the maximum level of resolution for Haar wavelet. The wavelet number** i **and the parameters** m **and** k **have the relation** $i = m + k + 1$**. Equation** (2.21) **is valid for** $i \geq 3$**.**
The scaling functions for the family of Haar wavelets corresponding to $i = 1$, **and** $i = 2$ **are given by:**

$$h_1(x) = \begin{cases} 1, & \textbf{if } \ x \in [a, b); \\ 0, & \textbf{otherwise}, \end{cases} \tag{2.22}$$

and

$$h_2(x) = \begin{cases} 1, & \textbf{if } \ x \in [a, \frac{a+b}{2}); \\ -1, & \textbf{if } \ x \in [\frac{a+b}{2}, b); \\ 0, & \textbf{otherwise}. \end{cases} \tag{2.23}$$

Any function $y(x)$ **defined over the interval** (a, b) **can be decomposed as:**

$$y(x) = \sum_{i=0}^{\infty} c_i h_i(x), \tag{2.24}$$

where $c_i = \langle y(x), h_i(x) \rangle$**, here** $\langle . \rangle$ **stands for the inner product. In practice, only the first** m **terms are considered, where** m **is a power of 2, that is**

$$y(x) \cong u_m(x) = \sum_{i=0}^{m-1} c_i h_i(x)$$

with matrix form as:

$$y(x) \cong u_m(x) = C_m^T H_m(x), \tag{2.25}$$

where

$$C_m = [c_0, c_1, c_2, \cdots, c_{m-1}]^T \text{ and } H_m(x) = [h_0(x), h_1(x), h_2(x), \cdots, h_{m-1}(x)]^T.$$

2.5.1 ψ-Haar wavelets operational matrix

The ψ-Haar wavelet operational matrix of integration $P^{\alpha,\psi}$ of fractional order α is constructed and utilized for numerical approximation of ψ-fractional differential equations. We use equation (2.4.1) for the ψ- fractional integration of Haar wavelets. The generalized ψ-fractional integration of the Haar wavelets, $H_m = [h_0, h_1, h_2, \cdots, h_{m-1}]$, is given by:

$$P_i^{\alpha,\psi}(x) = \frac{1}{\Gamma(\alpha)} \int_a^x \psi'(t)\big(\psi(x) - \psi(t)\big)^{\alpha-1} h_i(t)dt. \tag{2.26}$$

These generalized ψ-fractional integrals can be approximated analytically as

$$P_i^{\alpha,\psi}(x) = \begin{cases} 0, & \text{if } x < \xi_1(i); \\ \frac{1}{\Gamma(\alpha+1)}\big[\psi(x) - \psi(\xi_1(i))\big]^{\alpha}, & \text{if } x \in [\xi_1(i), \xi_2(i)); \\ \frac{1}{\Gamma(\alpha+1)}\Big[\big(\psi(x) - \psi(\xi_1(i))\big)^{\alpha} - 2\big(\psi(x) - \psi(\xi_2(i))\big)^{\alpha}\Big], & \text{if } x \in (\xi_2(i), \xi_3(i)]; \\ \frac{1}{\Gamma(\alpha+1)}\Big[\big(\psi(x) - \psi(\xi_1(i))\big)^{\alpha} - 2\big(\psi(x) - \psi(\xi_2(i))\big)^{\alpha} + \\ \big(\psi(x) - \psi(\xi_3(i))\big)^{\alpha}\Big], & \text{if } x > \xi_3(i). \end{cases} \tag{2.27}$$

Equation (2.27) holds for $i > 1$, for $i = 1$ we have:

$$P^{\alpha,\psi}(x) = \frac{1}{\Gamma(\alpha+1)}\big[\psi(x) - \psi(a)\big]^{\alpha}. \tag{2.28}$$

Here we compute the ψ-Haar wavelets operational matrix $P^{\alpha,\psi}$ for the function $\psi(x) = x^2$ and $\alpha = 0.75$. The numerical and exact integration of the function $\psi(x) = x^3/15$ for $J = 5$ and different values of α is plotted in Figure 2.1.

$$P^{\alpha,\psi} = \begin{bmatrix} 0.4342 & -0.2816 & -0.0998 & -0.1763 & -0.0356 & -0.0623 & -0.0806 & -0.0953 \\ -0.0210 & 0.1735 & -0.0998 & 0.2392 & -0.0356 & -0.0623 & 0.1297 & 0.1153 \\ -0.0739 & 0.0653 & 0.0613 & -0.0204 & -0.0356 & 0.0833 & -0.0173 & -0.0058 \\ 0.0653 & -0.0653 & 0 & 0.1167 & 0 & 0 & -0.1051 & 0.1635 \\ -0.0285 & 0.0022 & 0.0221 & -0.00291 & 0.0211 & -0.0066 & -0.0019 & -0.0010 \\ -0.0094 & 0.0318 & -0.0224 & -0.00901 & 0 & 0.0435 & -0.0088 & -0.0020 \\ 0.0064 & -0.0064 & 0 & 0.06786 & 0 & 0 & 0.0616 & -0.0113 \\ 0.0280 & -0.0280 & 0 & -0.05604 & 0 & 0 & 0 & 0.0779 \end{bmatrix}.$$

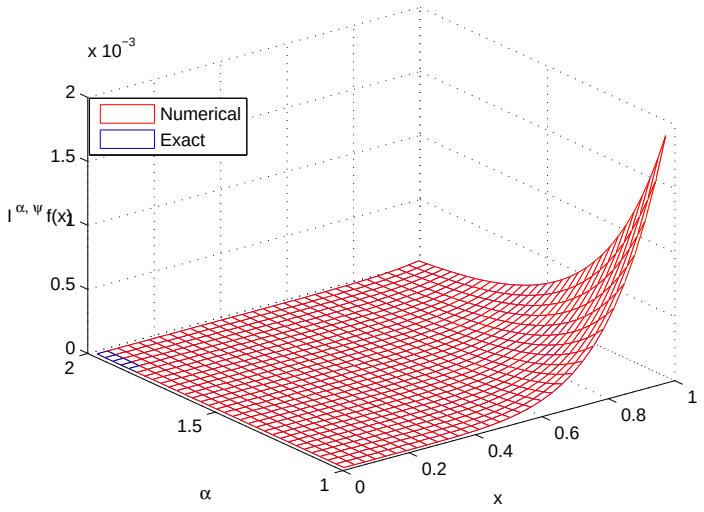

Figure 2.1: Numerical and exact integral of function $f(x) = \psi(x) = x^3/15$ for $J = 5$ and for different values of α.

2.6 Error analysis

Recently, Caputo type fractional differential equations are analyzed for error in [54]. Also, convergence for the solution of nonlinear Fredholm integral equation using Haar wavelet is given in [55]. We derive the upper bound for the error estimate using the $\psi-$Caputo fractional differential operator in Theorem 2.6.1 and Theorem 2.6.2 which are given in [56], showing convergence of the ψ-Haar wavelet method for fractional differential equations.

Theorem 2.6.1. *Suppose that $D^n y$ is continuous on $[a,b]$, assume also that there exists $M > 0$ such that $|D^{n,\psi} y(x)| \leq M$ for all $x \in [a,b]$, where $a, b \in \mathbb{R}^+$, $D^{n,\psi} y(x) = \left(\frac{1}{\psi'(x)}\frac{d}{dx}\right)^n y(x)$ and $D_a^{\alpha,\psi} y_m(x)$ is the approximation of $D_a^{\alpha,\psi} y(x)$, then we have*

$$\left\| D_a^{\alpha,\psi} y(x) - D_a^{\alpha,\psi} y_m(x) \right\|_E \leq \frac{(b-a)M\left(\psi'(b)\right)^{n-\alpha}}{\Gamma(n-\alpha+1)} \frac{1}{m^{(n-\alpha)}} \frac{1}{[1-2^{2(\alpha-n)}]^{1/2}}.$$

Proof. The function $D_a^{\alpha,\psi} y$ defined over the interval $[a,b]$ can be approximated as:

$$D_a^{\alpha,\psi} y(x) = \sum_{i=a}^{\infty} c_i h_i(x),$$

where

$$c_i = \langle D_a^{\alpha,\psi} y(x), h_i(x) \rangle = \int_a^b \left(D_a^{\alpha,\psi} y(x) \right) h_i(x) dx. \tag{2.29}$$

Suppose that $D_a^{\alpha,\psi} y_m$ is the following approximation of $D_a^{\alpha,\psi} y$

$$D_a^{\alpha,\psi} y_m(x) = \sum_{i=0}^{m-1} c_i h_i(x), \tag{2.30}$$

where $m = 2^{\beta+1}$, $\beta = 1, 2, 3, \cdots$, then

$$D_a^{\alpha,\psi} y(x) - D_a^{\alpha,\psi} y_m(x) = \sum_{i=m}^{\infty} c_i h_i(x) = \sum_{i=2^{\beta+1}}^{\infty} c_i h_i(x), \tag{2.31}$$

which implies that

$$\begin{aligned} \left\| D_a^{\alpha,\psi} y(x) - D_a^{\alpha,\psi} y_m(x) \right\|_E^2 &= \int_a^x \left(D_a^{\alpha,\psi} y(x) - D_a^{\alpha,\psi} y_m(x) \right)^2 dx \\ &= \sum_{i=2^{\beta+1}}^{\infty} \sum_{i'=2^{\beta+1}}^{\infty} c_i c_{i'} \int_a^x h_i(x) h_{i'}(x) dx. \end{aligned}$$

By orthogonality of the sequence $\{h_m(x)\}$, we have $\int_a^b h_m(x) h_m(x) dx = I_m$, where I_m is the identity matrix of order m, therefore,

$$\left\| D_a^{\alpha,\psi} y(x) - D_a^{\alpha,\psi} y_m(x) \right\|_E^2 = \sum_{i'=2^{\beta+1}}^{\infty} c_i^2. \tag{2.32}$$

From equation (2.29) we have:

$$\begin{aligned} c_i &= \int_a^b \left(D_a^{\alpha,\psi} y(x) \right) h_i(x) dx \\ &= 2^{\frac{j}{2}} \left\{ \int_{a+(b-a)k2^{-j}}^{a+(b-a)(k+\frac{1}{2})2^{-j}} D_a^{\alpha,\psi} y(x) dx - \int_{a+(b-a)(k+\frac{1}{2})2^{-j}}^{a+(b-a)(k+1)2^{-j}} D_a^{\alpha,\psi} y(x) dx \right\}. \end{aligned} \tag{2.33}$$

Using mean value theorem of integrals: there exist $x_1, x_2 \in (a, b)$ with

$$\begin{aligned} a + (b-a)k2^{-j} < x_1 < a + (b-a)\big(k + \frac{1}{2}\big)2^{-j}, \\ a + (b-a)\big(k + \frac{1}{2}\big)2^{-j} < x_2 < a + (b-a)(k+1)2^{-j}, \end{aligned}$$

such that

$$\begin{aligned} c_i =& 2^{\frac{j}{2}}(b-a) \Bigg\{ \left(a + (k + \frac{1}{2})2^{-j} \quad - \quad (a + k2^{-j}) \right) D_a^{\alpha,\psi} y(x_1) \\ & - \left(a + (k+1)2^{-j} - (a + (k + \frac{1}{2})2^{-j} \right) D_a^{\alpha,\psi} y(x_2) \Bigg\} \\ =& 2^{\frac{j}{2}}(b-a) \left\{ 2^{-j-1} \left(D_a^{\alpha,\psi} y(x_1) - D_a^{\alpha,\psi} y(x_2) \right) \right\}. \end{aligned} \tag{2.34}$$

Hence

$$c_i^2 = 2^{-j-2}(b-a)^2(D_a^{\alpha,\psi}y(x_1) - D_a^{\alpha,\psi}y(x_2))^2. \tag{2.35}$$

Using the definition of ψ-Caputo differential operator,the increasing property of ψ and the condition $|D^{n,\psi}y(x)| \leq M$, we have:

$$\begin{aligned}
|D_a^{\alpha,\psi}y(x_1) - D_a^{\alpha,\psi}y(x_2)| =& \frac{1}{\Gamma(n-\alpha)}\bigg| \int_a^{x_1} \psi'(x)\Big(\psi(x_1)-\psi(x)\Big)^{n-\alpha-1} D^{n,\psi}y(x)dx \\
&- \int_a^{x_2} \psi'(x)\Big(\psi(x_2)-\psi(x)\Big)^{n-\alpha-1} D^{n,\psi}y(x)dx\bigg| \\
\leq& \frac{1}{\Gamma(n-\alpha)}\bigg| \int_a^{x_1} \psi'(x)\Big(\psi(x_1)-\psi(x)\Big)^{n-\alpha-1} D^{n,\psi}y(x)dx \\
&- \int_a^{x_1} \psi'(x)\Big(\psi(x_2)-\psi(x)\Big)^{n-\alpha-1} D^{n,\psi}y(x)dx\bigg| \\
&+ \bigg| \int_{x_1}^{x_2} \psi'(x)\Big(\psi(x_2)-\psi(x)\Big)^{n-\alpha-1} D^{n,\psi}y(x)dx\bigg|
\end{aligned}$$

$$\begin{aligned}
\leq& \frac{1}{\Gamma(n-\alpha)}\Bigg(\int_a^{x_1} \psi'(x)\bigg[\Big(\psi(x_1)-\psi(x)\Big)^{n-\alpha-1} - \Big(\psi(x_2)-\psi(x)\Big)^{n-\alpha-1}\bigg]\Big|D^{n,\psi}y(x)\Big|dx \\
&+ \int_{x_1}^{x_2} \psi'(x)\Big(\psi(x_2)-\psi(x)\Big)^{n-\alpha-1}\Big|D^{n,\psi}y(x)\Big|dx\Bigg), \text{where } n-\alpha-1>0 \\
=& \frac{M}{\Gamma(n-\alpha+1)}\Bigg(\Big(\psi(x_1)-\psi(a)\Big)^{n-\alpha} - \Big(\psi(x_2)-\psi(a)\Big)^{n-\alpha} + 2\Big(\psi(x_2)-\psi(x_1)\Big)^{n-\alpha}\Bigg).
\end{aligned}$$

Since $x_1 > a,\ x_2 > a$ and $x_2 > x_1$ and $\psi(x)$ is an increasing function, so $\Big(\psi(x_1)-\psi(a)\Big)^{n-\alpha} - \Big(\psi(x_2)-\psi(a)\Big)^{n-\alpha} < 0$. Therefore,

$$|D_a^{\alpha,\psi}y(x_1) - D_a^{\alpha,\psi}y(x_2)| \leq \frac{2M}{\Gamma(n-\alpha+1)}\Big(\psi(x_2)-\psi(x_1)\Big)^{n-\alpha}.$$

By mean value theorem, there exists $\xi \in [x_1, x_2] \subseteq [a,b]$ such that $\psi(x_2)-\psi(x_1) \leq (x_2-x_1)\psi'(\xi)$, we get:

$$\begin{aligned}
|D_a^{\alpha,\psi}y(x_1) - D_a^{\alpha,\psi}y(x_2)| &\leq \frac{2M}{\Gamma(n-\alpha+1)}\Big((x_2-x_1)\psi'(\xi)\Big)^{n-\alpha} \\
&\leq \frac{2M}{\Gamma(n-\alpha+1)2^{j(n-\alpha)}}\Big(\psi'(b)\Big)^{n-\alpha},
\end{aligned}$$

which implies that,

$$\left(D_a^{\alpha,\psi}y(x_1) - D_a^{\alpha,\psi}y(x_2)\right)^2 \leq \frac{4M^2}{\Gamma^2(n-\alpha+1)2^{2j(n-\alpha)}}\left(\psi^{'}(b)\right)^{2(n-\alpha)}. \tag{2.36}$$

By substituting the equation (2.36) in (2.35), we get:

$$c_i^2 \quad \leq 2^{-j-2}(b-a)^2\frac{4M^2}{\Gamma^2(n-\alpha+1)2^{2j(n-\alpha)}}\left(\psi^{'}(b)\right)^{2(n-\alpha)}. \tag{2.37}$$

Combining equation (2.32) and equation (2.37), we get

$$\begin{aligned}\left\|D_a^{\alpha,\psi}y(x) - D_a^{\alpha,\psi}y_m(x)\right\|_E^2 &= \sum_{i=2^{\beta+1}}^{\infty} c_i^2 = \sum_{j=\beta+1}^{\infty}\left(\sum_{i=2^j}^{2^{j+1}-1} c_i^2\right)\\ \leq \sum_{j=\beta+1}^{\infty}(b-a)^2\frac{M^2}{\Gamma^2(n-\alpha+1)2^{2j(n-\alpha)+j}}&\left(\psi^{'}(b)\right)^{2(n-\alpha)}(2^{j+1}-1-2^j+1).\end{aligned} \tag{2.38}$$

$$\begin{aligned}&= \frac{(b-a)^2M^2\left(\psi^{'}(b)\right)^{2(n-\alpha)}}{\Gamma^2(n-\alpha+1)}\sum_{j=\beta+1}^{\infty}\frac{1}{2^{2j(n-\alpha)}}\\ &= \frac{(b-a)^2M^2\left(\psi^{'}(b)\right)^{2(n-\alpha)}}{\Gamma^2(n-\alpha+1)}\frac{1}{2^{2(\beta+1)(n-\alpha)}}\frac{1}{1-2^{2(\alpha-n)}}.\end{aligned}$$

Which implies that

$$\left\|D_a^{\alpha,\psi}y(x) - D_a^{\alpha,\psi}y_m(x)\right\|_E \leq \frac{(b-a)M\left(\psi^{'}(b)\right)^{n-\alpha}}{\Gamma(n-\alpha+1)}\frac{1}{2^{(\beta+1)(n-\alpha)}}\frac{1}{\left[1-2^{2(\alpha-n)}\right]^{\frac{1}{2}}}. \tag{2.39}$$

Using $m = 2^{\beta+1}$, (2.39) can also be written as:

$$\left\|D_a^{\alpha,\psi}y(x) - D_a^{\alpha,\psi}y_m(x)\right\|_E \leq \frac{(b-a)M\left(\psi^{'}(b)\right)^{n-\alpha}}{\Gamma(n-\alpha+1)}\frac{1}{K^{(n-\alpha)}}\frac{1}{\left[1-2^{2(\alpha-n)}\right]^{\frac{1}{2}}}. \tag{2.40}$$

The error bound can be computed once we get the value of M. For estimating M, since $D^n y(x)$ is bounded and continuous on the interval $[a,b]$, therefore, $D^{n,\psi}y(x)$ is also bounded and continuous in $[a,b]$ and can be estimated as:

$$D^{n,\psi}y(x) \cong \sum_{i=0}^{n-1} c_i h_i(x) = C_m^T H_m(x), \tag{2.41}$$

where $C_m = [c_0, c_1, c_2, \cdots, c_{m-1}]^T$ and $H_m(x) = [h_0(x), h_1(x), h_2(x), \cdots, h_{m-1}(x)]^T$. Integrating (2.41), we have:

$$D^{n-1,\psi}y(x) = \int_a^x D^{n,\psi}y(x)dx + D^{n-1,\psi}y(a) \cong C_m^T P^{1,\psi} H_m(x). \tag{2.42}$$

Similarly,

$$D^{m-2,\psi}y(x) = \int_a^x D^{n-1,\psi}y(x)dx + D^{n-2,\psi}y(a) \cong C_m^T P^{2,\psi} H_m(x). \tag{2.43}$$

Proceeding in the same way we get:

$$D^{\psi}y(x) \cong C_m^T P^{n,\psi} H_m(x). \tag{2.44}$$

By defining the points $x_j = \frac{j-1/2}{n}, \quad j = 0, 1, 2, \cdots, n$. Substituting x_j in (2.44), we have:

$$D^{\psi}y(x_j) \cong C_m^T P^{n,\psi} H_m(x_j). \tag{2.45}$$

The matrix form of (2.45) is as:

$$D^{\psi}Y^T \cong C_m^T P^{n,\psi} H_m(x_j), \tag{2.46}$$

where $D^{\psi}Y^T = [D^{\psi}y(x_1), D^{\psi}y(x_2), D^{\psi}y(x_3), \cdots, D^{\psi}y(x_m)]^T$. By solving equation (2.46), we can find C_m^T. From equation (2.41), we know the value of $D^{n,\psi}(x)$ for each $x \in [a, b]$. Assume $t_i \in [a, b]$, for $i = 1, 2, 3, \cdots, l$, $t_i = (i-1)/l$ and calculate $D^{n,\psi}y(t_i)$ for $i = 1, 2, 3, \ldots, l$, then $\varepsilon + \max|D^n y(t_i)|$ may be considered as the estimation for M. Clearly, this estimation would come more precise if l increases and ε be chosen as b. □

Theorem 2.6.2. *Suppose that the function $D_a^{\alpha,\psi}y_m$, obtained by using ψ-Haar wavelets is the approximation of $D_a^{\alpha,\psi}y$, then we have an exact upper bound as follows*

$$\left\|y(x) - y_m(x)\right\|_E \leq \frac{MN}{\Gamma(\alpha+1)\Gamma(n-\alpha+1)} \frac{1}{m^{(n-\alpha)}} \frac{1}{[1-2^{2(\alpha-n)}]^{\frac{1}{2}}}. \tag{2.47}$$

where $N = max|(b-a)(\psi(b))^{n-\alpha}(\psi(x)-\psi(0))^{\alpha}|$

The proof of the Theorem 2.6.2. can easily be established by using Theorem 2.6.1. From equation (2.47) **we can see that $\left\|y(x) - y_m(x)\right\|_E \to 0$ when $m \to \infty$. So we deduce that the ψ-Haar wavelets method is convergent.**

Example 2.6.1. To demonstrate the validity and applicability of error analysis and the upper bound, we consider the following fractional differential equation

$$D_0^{\alpha,\psi}y(x) + y(x) = (\psi(x))^2 + \frac{\Gamma(3)}{\Gamma(3-\alpha)}, \ 0 < \alpha \leq 1, \text{ and } x \in [0, 1].$$

Table 2.1. Error and upper bound of error for different values of J and $\alpha = 0.25$.

J	$\left\|y(x) - y_m(x)\right\|_E$	Upper bound of error
5	4.6000×10^{-4}	0.1274
6	1.9029×10^{-4}	0.0761
7	7.9228×10^{-5}	0.0453
8	3.3118×10^{-5}	0.0269

Subject to the initial condition $y(0) = y_0$, the exact solution is given by $y(x) = (\psi(x))^2$. The error and the upper bound of error computed for different values of $\alpha = 0.25$ are given in the Table 2.1, which shows that using the ψ-Haar wavelets method, we may obtain a good approximation of the exact solution. We might also observe that as J increases, the error gets smaller and smaller. The value of the upper bound of error is also getting smaller and smaller at the same time. It also demonstrates that, as J increases, the numerical solutions gradually approach the exact solution.

Chapter 3

Numerical solution of initial value problems using ψ-Haar wavelets method

In this chapter we find solutions for linear and nonlinear Fractional Differential Equations(FDEs) involving ψ-Caputo derivative. This chapter is based on our paper [56], where we have derived an operational matrix to find a numerical approximation of ψ- FDEs. We extended the method to nonlinear ψ-FDEs by using quasi linearization technique to linearize the nonlinear problems. The method is simple and good mathematical tool for finding solution of nonlinear ψ-FDEs. The operational matrix approach offers less computational complexity.

We give some numerical examples utilizing the ψ-Haar wavelet operational matrix method to approximate the numerical solutions of linear and non-linear initial value FDEs.

3.1 Linear problems

In this section, we take two linear problems as follows.

Example 3.1.1. Consider the linear fractional ordinary differential equation with variable coefficient involving ψ-Caputo derivative with initial condition

$$D_0^{\alpha,\psi} y + a(x)y = f(x),\ 0 < \alpha \leq 1,\ \text{and } x \in [0,1] \text{ with } y(0) = y_0. \tag{3.1}$$

For $a(x) = e^x$ and $f(x) = e^x(\psi(x))^{2\alpha} + \Gamma(2\alpha+1)/\Gamma(\alpha+1)(\psi(x))^{\alpha}$, it is easy to verify that $y(x) = (\psi(x))^{2\alpha}$ is the analytic solution of equation (3.1). To find the approximate

solution, we apply the ψ-Haar wavelet technique to equation (3.1). Consider

$$D_0^{\alpha,\psi} y(x) = C_m^T H_m(x). \tag{3.2}$$

Applying the integral operator $\mathcal{I}_0^{\alpha,\psi}$ on both sides of equation (3.2), we have

$$y(x) = \mathcal{I}_0^{\alpha,\psi} C_m^T H_m(x) + c_1 = C_m^T P_{m\times m}^{\alpha,\psi} H_m(x) + c_1. \tag{3.3}$$

Using the initial condition in (3.1), we have:

$$y(x) = C_m^T P_{m\times m}^{\alpha,\psi} H_m(x) + (\psi(0))^{2\alpha}. \tag{3.4}$$

Substituting (3.2) and (3.4) in (3.1), we have:

$$C_m^T \big(H_m + a(x) P_{m\times m}^{\alpha,\psi} H_m(x)\big) = f(x) - a(x)(\psi(0))^{2\alpha}. \tag{3.5}$$

Consider the diagonal matrix A of the of the function $a(x)$ at the collocation points $x_i = \frac{2i-1}{2m}x$, where $i = 1,\ 2,\ \cdots,\ m$, is given by:

$$A = \begin{bmatrix} a(x_1) & 0 & \cdots & 0 \\ 0 & a(x_2) & \cdots & 0 \\ \vdots & \vdots & \ddots & \vdots \\ 0 & 0 & \cdots & a(x_m) \end{bmatrix}.$$

From equation (3.5), we have the following matrix form:

$$C_m^T \big(H_m + A P_{m\times m}^{\alpha,\psi} H_m\big) = F, \tag{3.6}$$

where $F = f(x) - a(x)(\psi(0))^2$. To find the value of C we have to solve the algebraic system (3.6), and putting the value of C into (3.4) we will get the approximate solution. Numerical solutions are obtain for different values of α and J, which are shown in the tabular form in the Table 3.1. Numerical solution of equation (3.1) for $\psi(x) = x^2$ and $\psi(x) = \tan(x/2)$, and different values of α is shown in the graphical form in the Figure 3.1. The exact and approximate solution and the maximum absolute error for $J = 6$ and $\alpha = 1$ are given in the Figure 3.2 (a) and (b) respectively.

Example 3.1.2. Consider the initial value problem with variable coefficients

$$D_0^{\alpha,\psi} y + a(x) D_0^{\beta,\psi} y + b(x) y = f(x), \tag{3.7}$$

where $1 < \alpha \leq 2$, $0 < \beta \leq 1$ and $x \in [0, 1]$, with the initial conditions

$$y(0) = y_0, \qquad y^{'}(0) = y_1. \tag{3.8}$$

Table 3.1. Maximum absolute error for different values of α and J.

J	$\alpha = 0.5$	$\alpha = 0.7$	$\alpha = 0.9$	$\alpha = 1.0$
5	2.383349×10^{-4}	1.936029×10^{-4}	1.825123×10^{-4}	1.892904×10^{-4}
6	8.449661×10^{-5}	5.876715×10^{-5}	4.819711×10^{-5}	4.732614×10^{-5}
7	2.991332×10^{-5}	1.787101×10^{-5}	1.273172×10^{-5}	1.183166×10^{-5}
8	1.058271×10^{-5}	5.444213×10^{-6}	3.365286×10^{-6}	2.957938×10^{-6}

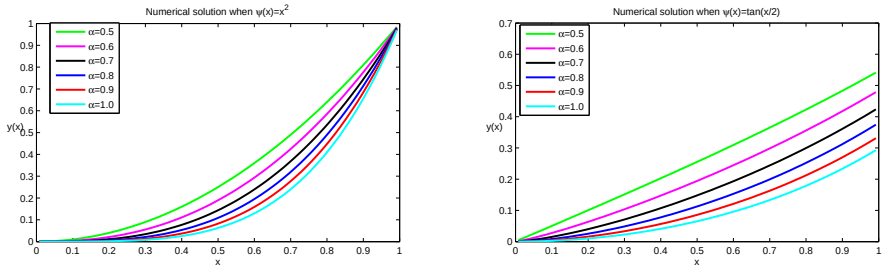

Figure 3.1: Numerical solutions of equation (3.1) for $J = 8$ and for different values of α.

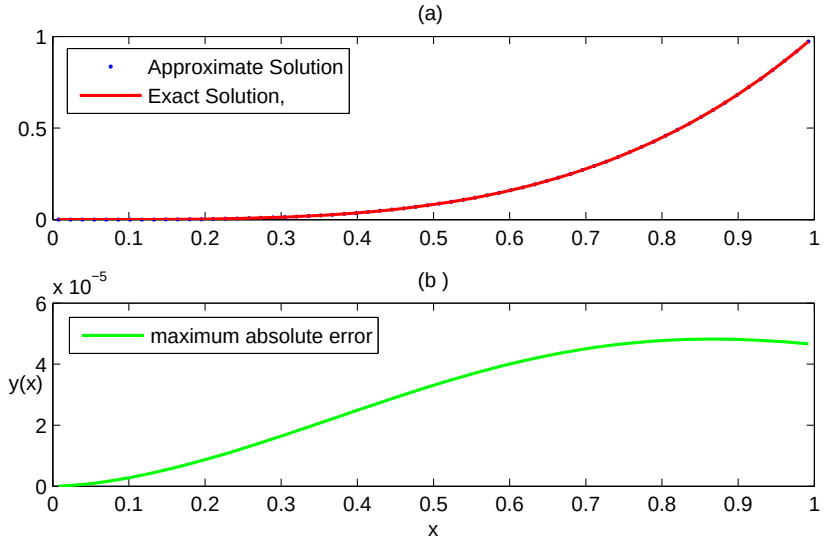

Figure 3.2: For $J = 6$, $\alpha = 1$ and $\psi(x) = x^2$ (a) exact and approximate solution (b) maximum absolute error

For $a(x) = e^x$, $b(x) = \sin(x)$, and

$$f(x) = \frac{\Gamma(3)}{\Gamma(3-\alpha)}(\psi(x))^{2-\alpha} + a(x)\frac{\Gamma(3)}{\Gamma(3-\beta)}(\psi(x))^{2-\beta} + b(x)(\psi(x))^2.$$

One may verify that $y(x) = (\psi(x))^2$ is the analytic solution for the problem (3.7). For approximate solution, we use Haar wavelet techniques. Let

$$D_0^{\alpha,\psi} y(x) = C_m^T H_m(x). \tag{3.9}$$

Applying the integral operator $\mathcal{I}_0^{\alpha,\psi}$ on both sides of equation (3.9), we obtain

$$y(x) = \mathcal{I}_0^{\alpha,\psi} C_m^T H_m(x) + c_1 + c_2(\psi(x) - \psi(0)). \tag{3.10}$$

Using the initial conditions in (3.10),we get $c_1 = y_0$ and $c_2 = y_1/(\psi(0))'$. Equation (3.10) becomes

$$y(x) = C_m^T P^{\alpha,\psi} H_m + y_0 + y_1/(\psi(0))'(\psi(x) - \psi(0)). \tag{3.11}$$

Again applying the operator $D_0^{\beta,\psi}$ on (3.11) we get

$$D_0^{\beta,\psi} y = C_m^T P^{\alpha-\beta} H_m + y_1/(\psi(0))' \Gamma(2)/\Gamma(2-\beta)(\psi(x))^{1-\beta}. \tag{3.12}$$

Substituting equations (3.9), (3.10) and (3.12) in equation (3.7), we get

$$C_m^T (H_m + a(x) P^{\alpha-\beta,\psi} H_m + b(x) P^{\alpha,\psi} H_m) = F(x), \tag{3.13}$$

where $F(x) = f(x) - a(x)\Gamma(2)/\Gamma(2-\beta)(\psi(x))^{1-\beta} - b(x)(\psi(x))^2$. Solving equation (3.13) for C and putting the value of C in equation (3.11) we get the required solution. Exact and numerical solutions and their maximum absolute error are presented in the Figure 4.4 for $J = 6$ and various values of α. Maximum absolute error obtained for different values of α, β and J are shown in the tabular form in the Table 3.2. We observed that maximum absolute error decrease by increasing value of J.

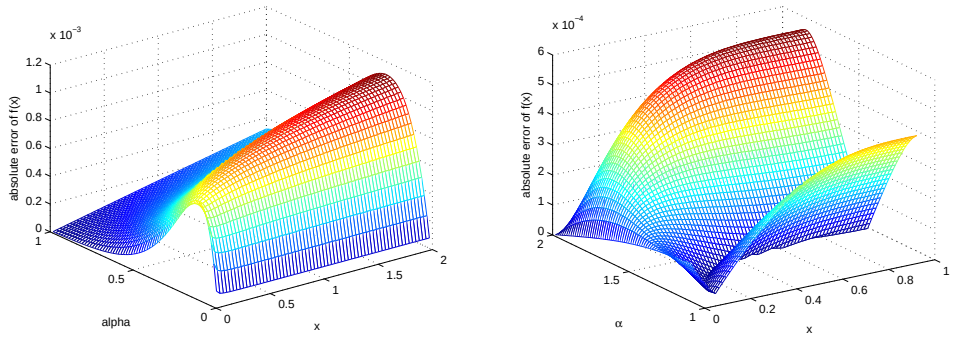

Figure 3.3: Exact and numerical solutions of equation (3.7) for different values of α and their absolute error.

Table 3.2. Maximum absolute error for different values of α, β and J.

		$\beta = 0.7$		
α	$J = 5$	$J = 6$	$J = 7$	$J = 8$
1.5	3.503526×10^{-4}	1.215296×10^{-4}	4.273888×10^{-5}	1.514266×10^{-5}
1.6	5.026274×10^{-4}	1.901886×10^{-4}	7.221228×10^{-5}	2.744912×10^{-5}
1.7	6.705020×10^{-4}	2.719547×10^{-4}	1.104044×10^{-4}	4.483553×10^{-5}
1.8	7.818761×10^{-4}	3.392458×10^{-4}	1.473415×10^{-4}	6.403718×10^{-5}
1.9	6.757137×10^{-4}	3.139957×10^{-4}	1.46089×10^{-4}	6.803371×10^{-5}
		$\beta = 0.9$		
1.5	2.718617×10^{-4}	9.020570×10^{-5}	3.072957×10^{-5}	1.067530×10^{-5}
1.6	4.134163×10^{-4}	1.573446×10^{-4}	6.052547×10^{-5}	2.337513×10^{-5}
1.7	5.949382×10^{-4}	2.449613×10^{-4}	1.008262×10^{-4}	4.142341×10^{-5}
1.8	7.228608×10^{-4}	3.170263×10^{-4}	1.387916×10^{-4}	6.066605×10^{-5}
1.9	6.334264×10^{-4}	2.960765×10^{-4}	1.382828×10^{-4}	6.455392×10^{-5}

3.2 Nonlinear problems

Example 3.2.1. Consider the non-linear ψ-Caputo fractional differential equation:

$$D_0^{\alpha,\psi} y + y^2 = f(x), \quad 0 < \alpha \leq 1, \quad x \in [0,1] \quad \text{and} \quad y(0) = y_0. \tag{3.14}$$

For $f(x) = e^x(\psi(x))^2 + \Gamma(3)/\Gamma(3-\alpha)(\psi(x))^{2-\alpha}$ it is easy to verify that $y(x) = (\psi(x))^2$ is the exact solution of equation (3.14). To find the approximate solution we first apply the quasilinearization techniques [57] to linearize the nonlinear terms in equation (3.14) and then utilize Haar wavelet technique to obtain the approximate solution of the linear problem. The linearized form of (3.14) is

$$D_0^{\alpha,\psi} y_{r+1} + 2y_r y_{r+1} = f(x) + y_r^2. \tag{3.15}$$

Let

$$D_0^{\alpha,\psi} y_{r+1} = C_m^T H_m. \tag{3.16}$$

Applying the integral operator $\mathcal{I}_0^{\alpha,\psi}$ on both sides of equation (3.16), we have

$$y_{r+1} = \mathcal{I}^{\alpha,\psi} C_m^T H_m(x) + c_1 = C_m^T P_0^{\alpha,\psi} H_m(x) + c_1. \tag{3.17}$$

Using the initial condition in (3.17), we have

$$y_{r+1} = C_m^T P_{m\times m}^{\alpha,\psi} H_m(x) + (\psi(0))^2. \tag{3.18}$$

Substituting (3.16) and (3.17) in (3.15) we have,

$$C_m^T\big(H_m + 2y_r P_{m\times m}^{\alpha,\psi} H_m\big) = f(x) + y_r^2 - y_0. \tag{3.19}$$

From equation (3.19) we will have the following matrix form

$$C_m^T\big(H_m + 2y_r P_{m\times m}^{\alpha,\psi} H_m\big) = F, \tag{3.20}$$

where $F = f(x) + y_r^2 - y_0$. To find the value of C we have to solve the algebraic system (3.20), and putting the value of C into (3.18) we will get the approximate solution at the collocation points. Maximum absolute error for $\psi(x) = x^3$ are given in the Table 3.3. Also the numerical solutions for various functions ψ are displayed in the graphical form in the Figure 3.4. Moreover, for $J = 6$, $\alpha = 1$ and $\psi(x) = x^2 - x$, the exact and numerical solutions and their maximum absolute error are presented in the Figure 3.5.

Table 3.3. maximum absolute error for $\psi(x) = x^3$ and different values of J and α.

J	$\alpha = 0.6$	$\alpha = 0.7$	$\alpha = 0.8$	$\alpha = 0.9$	$\alpha = 1.0$
5	1.99059×10^{-3}	1.60809×10^{-3}	1.25456×10^{-3}	9.49891×10^{-4}	7.00046×10^{-4}
6	6.39868×10^{-4}	4.82375×10^{-4}	3.52569×10^{-4}	2.51551×10^{-4}	1.76100×10^{-4}
7	2.05770×10^{-4}	1.44594×10^{-4}	9.88581×10^{-5}	6.63693×10^{-5}	4.41123×10^{-5}
8	6.64110×10^{-5}	4.34549×10^{-5}	2.77479×10^{-5}	1.75011×10^{-5}	1.10358×10^{-5}
9	2.15209×10^{-5}	1.31026×10^{-5}	7.80338×10^{-6}	4.61656×10^{-6}	2.75975×10^{-6}

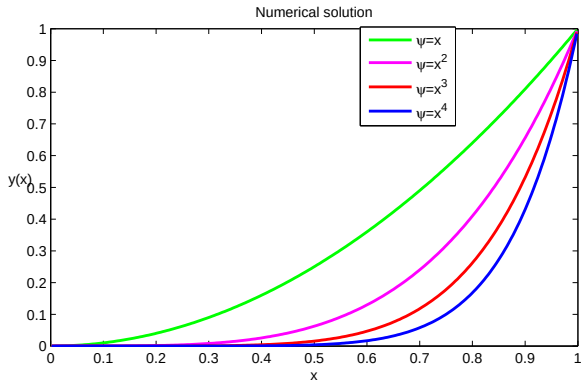

Figure 3.4: Numerical solutions for $\alpha = 1,\ J = 8$ and for different functions $\psi(x)$.

Example 3.2.2. Consider the nonlinear ψ-Caputo fractional differential equation with variable coefficients

$$D_0^{\alpha,\psi} y + a(x) D_0^{\beta,\psi} y + y D_0^{\gamma,\psi} y = f(x), \tag{3.21}$$
$$1 < \alpha \leq 2,\ 0 < \beta \leq 1,\ 0 < \gamma \leq 1 \text{ and } x \in [0, 1].$$

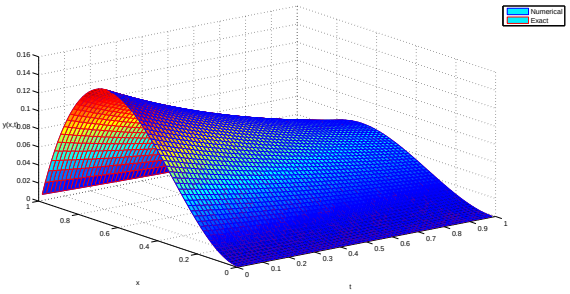

Figure 3.5: for $J = 6$, $\alpha = 1$ and $\psi(x) = x^2 - x$ (1) the exact and approximate solution (2) the maximum absolute error between exact and approximate solution

$$y(0) = y_0, \quad y'(0) = y_1. \tag{3.22}$$

For $a(x) = x^2$ and $f(x) = 2/\Gamma(3-\alpha)\ (\psi(x))^{2-\alpha} + a(x)2/\Gamma(3-\beta)\ (\psi(x))^{2-\beta}$ $+2(\psi(x))^2/\Gamma(3-\gamma)\ (\psi(x))^{2-\gamma}$. One may verify that $y(x) = (\psi(x))^2$ is the analytic solution for the problem (3.21). For linearization of the nonlinear terms we use the Quasilinearization techniques and then apply the ψ-Haar wavelet method to find the approximate solution of the linearized fractional differential equation. The linearized form of (3.21) becomes

$$D_0^{\alpha,\psi} y_{r+1} + a(x) D_0^{\beta,\psi} y_{r+1} + (D_0^{\gamma,\psi} y_r) y_{r+1} + (y_r) D_0^{\gamma,\psi} y_{r+1} = f(x) - y_r D_0^{\gamma,\psi} y_r. \tag{3.23}$$

Consider

$$D_0^{\alpha,\psi} y_{r+1} = C_m^T H_m \tag{3.24}$$

applying the integral operator $\mathcal{I}_0^{\alpha,\psi}$ on both sides of (3.24)

$$y_{r+1} = \mathcal{I}_0^{\alpha,\psi} C_m^T H_m(x) + c_1 + c_2(\psi(x) - \psi(0)) \tag{3.25}$$

using the initial conditions from equation (3.22) in equation (3.25) we get $c_1 = y_0$ and $c_2 = y_1/(\psi(0))'$. Using values of c_1 and c_2 in equation (3.25) we get,

$$y_{r+1} = C_m^T P^{\alpha,\psi} H_m + y_0 + y_1/(\psi(0))'(\psi(x) - \psi(0)) \tag{3.26}$$

applying the operator $D_0^{\beta,\psi}$ on equation (3.26) we get

$$D_0^{\beta,\psi} y_{r+1} = C_m^T P^{\alpha-\beta} H_m + y_1/(\psi(0))'\Gamma(2)/\Gamma(2-\beta)(\psi(x))^{1-\beta} \tag{3.27}$$

again applying the operator $D^{\gamma,\psi}$ on equation (3.26) we get

$$D_0^{\gamma,\psi} y_{r+1} = C_m^T P^{\alpha-\gamma} H_m + y_1/(\psi(0))'\Gamma(2)/\Gamma(2-\gamma)(\psi(x))^{1-\gamma} \tag{3.28}$$

substituting equations (3.24), (3.26), (3.27) and (3.28) in equation (3.21), we get

$$C_m^T(H_m + a(x)P^{\alpha-\beta,\psi}H_m + (D_0^{\gamma,\psi}y_r)P^{\alpha,\psi}H_m + (y_r)P^{\alpha-\gamma,\psi}) = F(x). \tag{3.29}$$

solving equation (3.29) for C and putting the value of C in equation (3.26) we get the required numerical solutions. Table 3.4 contains the Maximum absolute error for distinct values of α and J. It shows that the maximum absolute error becomes smaller and smaller by taking greater values of J.

Table 3.4. Maximum absolute error for different values of α, β and J.

		$\beta = 0.5$ and $\gamma = 0.75$		
α	$J = 5$	$J = 6$	$J = 7$	$J = 8$
1.5	6.508129×10^{-5}	2.491141×10^{-5}	8.232340×10^{-6}	2.560913×10^{-6}
1.6	3.977282×10^{-5}	1.311337×10^{-5}	3.885524×10^{-6}	1.100174×10^{-6}
1.7	3.101982×10^{-5}	8.657270×10^{-6}	2.280651×10^{-6}	5.852983×10^{-7}
1.8	2.919557×10^{-5}	7.456689×10^{-6}	1.857814×10^{-6}	4.579923×10^{-7}
1.9	2.368181×10^{-5}	5.937789×10^{-6}	1.473492×10^{-6}	3.644554×10^{-7}

3.3 ψ-Fractional Relaxation Oscillation Differential Equations (ψ-FRODEs)

In this section, based on our paper [58], we present several examples of how to get numerical solutions of ψ-FRODEs using the ψ-HW operational matrix approach.

Example 3.3.1. Consider the ψ-FRODE:

$$D^{\alpha,\psi}y(x) + ay(x) = g(x), \quad 0 < \alpha \leq 1, \quad x \in [0,1] \quad \text{and} \quad y(0) = 0. \tag{3.30}$$

For $a = \frac{2}{\Gamma(3-\alpha)}$ $g(x) = \frac{2}{\Gamma(3-\alpha)}(\psi(x))^{2-\alpha} + (\psi(x)^2)$, the actual solution of equation (3.30) is $y(x) = (\psi(x))^2$. We use the ψ-HW technique to solve problem (3.30).
Let

$${}^{C}D^{\alpha,\psi}y(x) = C_m^T H_m(x). \tag{3.31}$$

Integrating equation (3.31) with respect to $\mathcal{I}_a^{\alpha,\psi}$ and using the initial conditions, we have

$$y(x) = \mathcal{I}^{\alpha,\psi}C_m^T H_m(x) = C_m^T P_{m\times m}^{\alpha,\psi} H_m(x). \tag{3.32}$$

Substituting (3.31) and (3.32) in (3.30) we have,

$$C_m^T\big(H_m(x) + aP_{m\times m}^{\alpha,\psi}H_m(x)\big) = g(x). \tag{3.33}$$

Equation (3.33) has the following matrix form:

$$C_m^T\big(H_m(x) + aP_{m\times m}^{\alpha,\psi}H_m(x)\big) = G, \tag{3.34}$$

where G is the matrix representation of g at the collocation points. Solving the algebraic system given by equation (3.34) for C_m^T and substituting this value into equation (3.32) we will have the required numerical solution. In Table 3.5 the max. absolute-error is given for $J = 6$ and $\psi(x) = x^3$. Approximate solutions for $J = 6$, $\alpha = 0.5$ and different choices of the function ψ are plotted in Figure 3.6. Also actual and approximate results and the absolute error are given for $J = 6$, $\alpha = 0.8$ and $\psi(x) = 1/3(x^3 - x^2 - x)$ in Figure 3.6.

Example 3.3.2. Consider the composite ψ-FRODE

$$D^{\alpha,\psi}y(x) + by(x) = \frac{\Gamma(2\alpha+1)}{\Gamma(\alpha+1)}(\psi(x))^{\alpha}\big[1 + (\psi(x))^{\alpha}\big], \quad 0 < \alpha \leq 1, \quad x \in [0,1]. \tag{3.35}$$

$$y(0) = 0. \tag{3.36}$$

For $b = \Gamma(2\alpha+1)/\Gamma(\alpha+1)$. The exact solution for the problem (3.35) is $y(x) = (\psi(x))^{2\alpha}$. For numerical solution we employ the ψ-HW technique. Let

$${}^{C}D^{\alpha,\psi}y(x) = C_m^T H_m(x). \tag{3.37}$$

Table 3.5. max absolute-error for various choices of α and J.

α	$J=5$	$J=6$	$J=7$	$J=8$	$J=9$
0.6	1.0141×10^{-4}	3.2169×10^{-5}	1.0296×10^{-5}	3.3179×10^{-6}	1.0751×10^{-6}
0.7	9.2421×10^{-5}	2.7180×10^{-5}	8.0595×10^{-6}	2.4056×10^{-6}	7.2213×10^{-7}
0.8	7.8481×10^{-5}	2.1470×10^{-5}	5.9091×10^{-6}	1.6349×10^{-6}	4.5452×10^{-7}
0.9	6.3749×10^{-5}	1.6437×10^{-5}	4.2464×10^{-6}	1.0994×10^{-6}	2.8527×10^{-7}
1.0	5.3010×10^{-5}	1.3250×10^{-5}	3.3127×10^{-6}	8.2817×10^{-7}	2.0704×10^{-7}

Integrating equation (3.37) with respect to $\mathcal{I}_a^{\alpha,\psi}$ and utilizing the initial condition, we have:

$$y(x)=\mathcal{I}^{\alpha,\psi}C_m^TH_m(x)=C_m^TP_{m\times m}^{\alpha,\psi}H_m(x). \tag{3.38}$$

substituting equations (3.37) and (3.38) in equation (3.35), we get

$$C_m^T\big(H_m(x)+P_{m\times m}^{\alpha,\psi}H_m(x)\big)=g(x), \tag{3.39}$$

where $\frac{\Gamma(2\alpha+1)}{\Gamma(\alpha+1)}(\psi(x))^\alpha\big[1+(\psi(x))^\alpha\big]$. Equation (3.39) in matrix form is given as:

$$C_m^T\big(H_m(x)+P_{m\times m}^{\alpha,\psi}H_m(x)\big)=G. \tag{3.40}$$

where G is the matrix representation of $g(x)$. The required approximate solutions can be obtained by using the value of C_m^T from equation (3.40) in equation (3.38). The max absolute-error are tabulated for $\psi(x)=\frac{(x)^3}{5}$ and various choices of J and α in Table 3.6, which shows that the Maximum Absolute Error decreasing by increasing the values of J. Figure 3.7 represents approximate solutions for different choices of α. Also comparison of actual and approximate results and their absolute-error are displayed in Figure 3.7.

Table 3.6. max absolute-error for various choices of α and J.

α	$J=5$	$J=6$	$J=7$	$J=8$	$J=9$
0.6	1.2082×10^{-4}	3.9804×10^{-5}	1.3061×10^{-5}	4.2822×10^{-6}	1.4045×10^{-6}
0.7	9.1203×10^{-5}	2.8002×10^{-5}	8.5466×10^{-6}	2.6042×10^{-6}	7.9372×10^{-7}
0.8	6.7053×10^{-5}	1.9253×10^{-5}	5.4799×10^{-6}	1.5545×10^{-6}	4.4065×10^{-7}
0.9	4.8650×10^{-5}	1.3151×10^{-5}	3.5128×10^{-6}	9.3312×10^{-7}	2.4729×10^{-7}
1.0	3.5205×10^{-5}	9.0544×10^{-6}	2.2954×10^{-6}	5.7785×10^{-7}	1.4496×10^{-7}

Example 3.3.3. Consider the ψ-FRODE:

$$\begin{aligned}D^{\alpha,\psi}y(x)+y(x)&=1-4\psi(x)+5(\psi(x))^2\\&\quad-\frac{4}{\Gamma(2-\alpha)}(\psi(x))^{1-\alpha}+\frac{10}{\Gamma(3-\alpha)}(\psi(x))^{2-\alpha},\end{aligned} \tag{3.41}$$

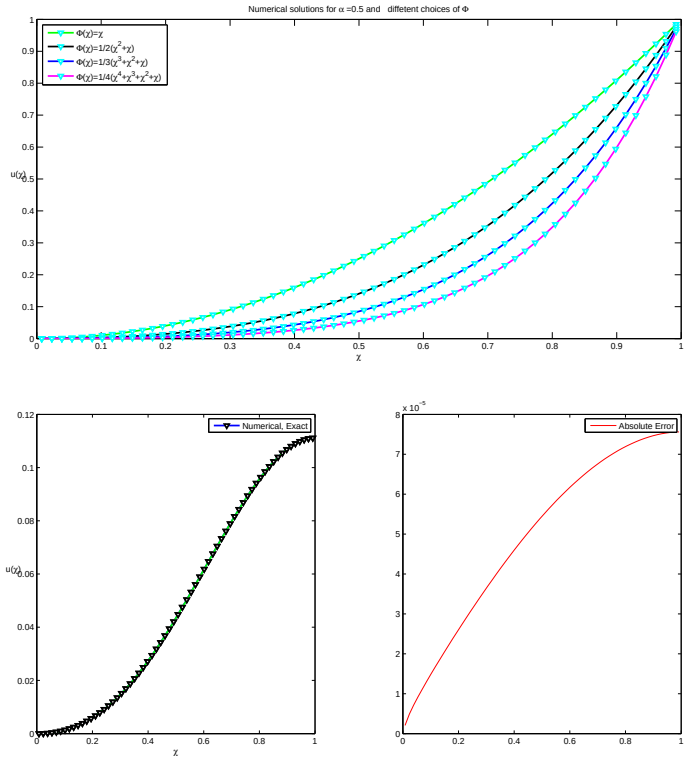

Figure 3.6: Approximate and Exact results of equation (3.30) and their absolute error.

where $0 < \alpha \leq 1$, $x \in [0, 1]$ and $y(0) = 1$. It is easy to verify that $y(x) = 1 - 4\psi(x) + 5(\psi(x))^2$ is the actual solution of equation (3.41). For numerical approximation we employ ψ-HW technique.
Let

$$ {}^{C}D^{\alpha,\psi}y(x) = C_m^T H_m(x). \tag{3.42}$$

Integrating equation (3.42) in terms of $\mathcal{I}_a^{\alpha,\psi}$ and using the initial conditions, we have

$$\begin{aligned} y(x) &= \mathcal{I}^{\alpha,\psi} C_m^T H_m(x) + y(0) \\ &= C_m^T P_{m\times m}^{\alpha,\psi} H_m(x) + 1. \end{aligned} \tag{3.43}$$

Substituting equations (3.42), (3.43) in equation (3.41) we have,

$$C_m^T \big(H_m(x) + P_{m\times m}^{\alpha,\psi} H_m(x)\big) = g(x), \tag{3.44}$$

where $g(x) = -4\psi(x) + 5(\psi(x))^2 - \frac{4}{\Gamma(2-\alpha)}(\psi(x))^{1-\alpha} + \frac{10}{\Gamma(3-\alpha)}(\psi(x))^{2-\alpha}$. The matrix form of equation (3.44) is:

$$C_m^T \big(H_m(x) + P_{m\times m}^{\alpha,\psi} H_m(x)\big) = G, \tag{3.45}$$

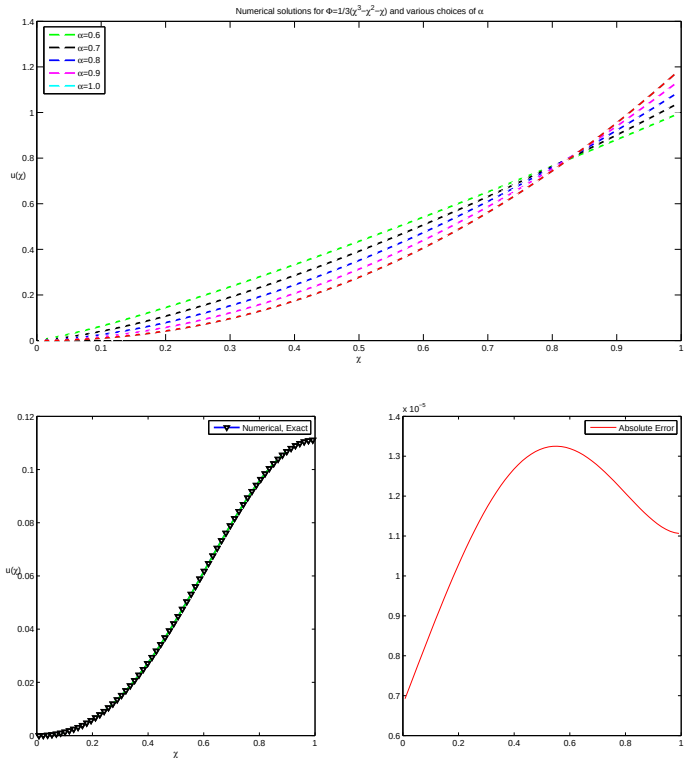

Figure 3.7: Approximate results of equation (3.35) for various choices of α, actual, approximate results and the absolute error.

where G is the matrix representation of $g(x)$. The required approximate solutions can be obtained by using the value of C_m^T from equation (3.45) in equation (3.43). Table 5.3 shows that the Maximum Absolute Error decreasing by increasing the values of J. Approximate solutions are displayed in Figure 5.3 for various values of ψ. Also Figure 5.3 represents approximate and exact solutions and their max absolute error for $\alpha = 0.75, J = 6$ and $\psi(x) = \frac{(x)^3}{15}$.

Table 3.7. max-absolute error for $\psi(x) = \frac{x^3}{15}$ and various choices of J and α.

α	$J=5$	$J=6$	$J=7$	$J=8$	$J=9$
0.6	9.0149×10^{-5}	2.9995×10^{-5}	9.9647×10^{-6}	3.3058×10^{-6}	1.0954×10^{-6}
0.7	4.3216×10^{-5}	1.3568×10^{-5}	4.2468×10^{-6}	1.3254×10^{-6}	4.1271×10^{-7}
0.8	1.5201×10^{-5}	4.5357×10^{-6}	1.3466×10^{-6}	3.9805×10^{-7}	1.1721×10^{-7}
0.9	2.2599×10^{-5}	6.0704×10^{-6}	1.5981×10^{-6}	4.1680×10^{-7}	1.0825×10^{-7}
1.0	2.2302×10^{-5}	5.7525×10^{-6}	1.4605×10^{-6}	3.6795×10^{-7}	9.2342×10^{-8}

Example 3.3.4. Consider the ψ-FRODE:

$$D^{\alpha,\psi}y(x) + \mu y(x) = g(x), \quad 0 < \alpha \leq 1, \quad x \in [0,1] \quad \text{and} \quad y(0) = 0. \tag{3.46}$$

For $\mu = 1$ and $g(x) = \frac{\Gamma(2\alpha+1)}{\Gamma(1+\alpha)}(\psi(x))^{\alpha} + \frac{\Gamma(2)}{\Gamma(2-\alpha)}(\psi(x))^{1+\alpha} + (\psi(x))^{2\alpha} + \psi(x)$ the exact solution of equation (3.46) is $(\psi(x))^{2\alpha} + \psi(x)$. For approximate solutions we use the ψ-HW technique. Let

$$^{C}D^{\alpha,\psi}y(x) = C_m^T H_m(x). \tag{3.47}$$

Integrating equation (3.47) with respect to $\mathcal{I}_0^{\alpha,\psi}$ and using the initial conditions, we have

$$y(x) = \mathcal{I}_0^{\alpha,\psi} C_m^T H_m(x) = C_m^T P_{m\times m}^{\alpha,\psi} H_m(x). \tag{3.48}$$

Substituting (3.47) and (3.48) in (3.46) we have,

$$C_m^T \big(H_m(x) + \mu P_{m\times m}^{\alpha,\psi} H_m(x)\big) = g(x). \tag{3.49}$$

Matrix representation of equation (3.49) is:

$$C_m^T \big(H_m(x) + \mu P_{m\times m}^{\alpha,\psi} H_m(x)\big) = G, \tag{3.50}$$

where G is the matrix representation of $g(x)$ at the collocation points.
Required approximate solutions can be obtained by using the value of C_m^T from equation (3.50) in equation (3.48). Table 5.4 shows that the Maximum Absolute Error decreasing by increasing the values of J. Also the Approximate solutions are displayed in Figure 5.4 for various values of α.

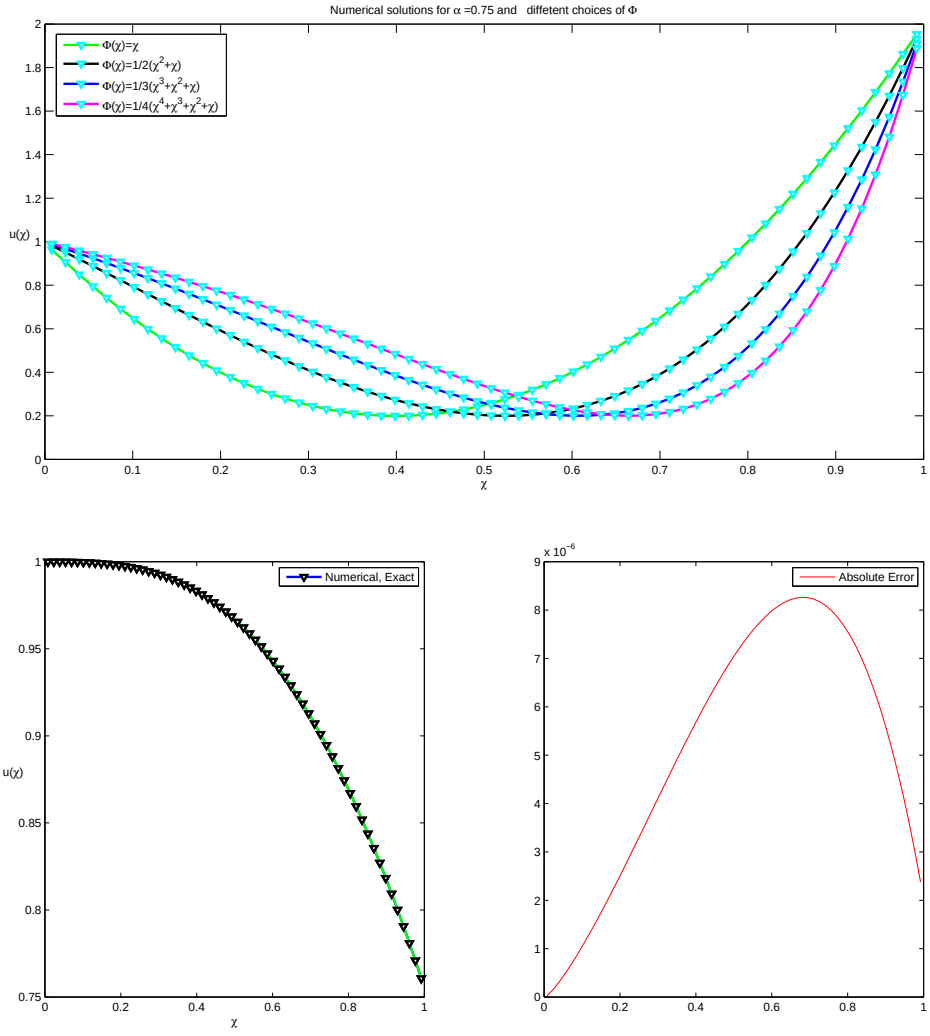

Figure 3.8: Approximate solutions for different choices of α and functions $\psi(x)$.

Table 3.8. max absolute-error for $\psi(x) = \frac{x^2}{15}$ and various choices of J and α.

α	$J = 5$	$J = 6$	$J = 7$	$J = 8$	$J = 9$
0.6	3.8255×10^{-5}	1.2688×10^{-5}	4.1987×10^{-6}	1.3876×10^{-6}	4.5829×10^{-7}
0.7	2.0382×10^{-5}	6.3431×10^{-6}	1.9679×10^{-6}	6.0937×10^{-7}	1.8843×10^{-7}
0.8	9.0481×10^{-6}	2.6383×10^{-6}	7.6857×10^{-7}	2.2372×10^{-7}	6.5069×10^{-8}
0.9	3.0670×10^{-6}	8.0025×10^{-7}	2.1048×10^{-7}	5.5848×10^{-8}	1.4938×10^{-8}
1.0	2.0360×10^{-6}	5.1692×10^{-7}	1.3022×10^{-7}	3.2678×10^{-8}	8.1852×10^{-9}

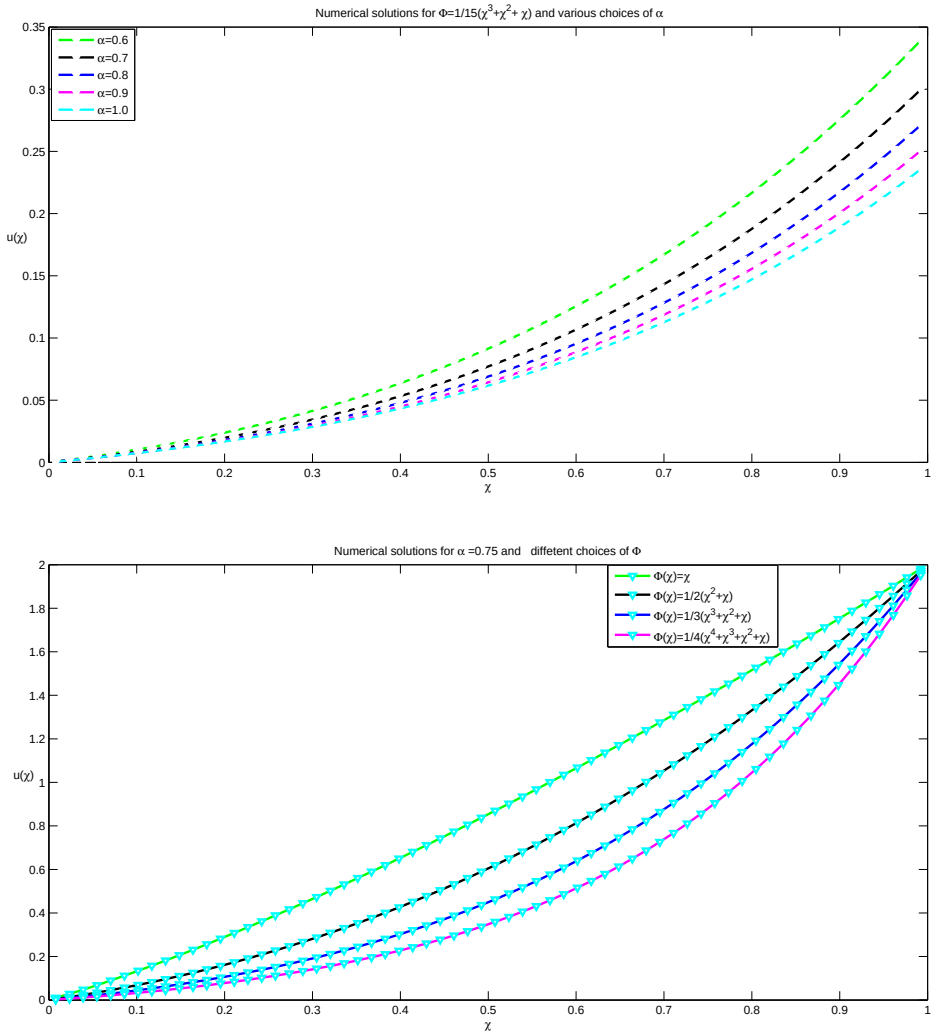

Figure 3.9: Numerical solutions for $\alpha = 1,\ J = 8$ and for different functions $\psi(x)$.

3.4 Conclusion

This chapter introduces a computational method for solving a class of fractional differential equations involving the ψ-Caputo fractional derivative based on a new operational-matrix of fractional integration, the ψ-HW operational-matrix.The method's convergence is demonstrated. The method can also be applied to other wavelet bases, such as Legendre, Chebyshev, and Gegenbauer wavelets.This approach can be applied to boundary value problems in FDEs as well as fractional partial differential equations.

Chapter 4

Numerical Solution of boundary value problems using ψ-Haar wavelet method

In this chapter we introduce a new numerical approach for solving linear and non-linear boundary value problems for ψ-fractional differential equations (ψ-FDEs) [59]. This approach relies on the ψ-Haar wavelet operational integration matrices. The ψ-operational matrices (ψ-OMs) are used to convert the ψ-FDE to an algebraic system of equations. The non-linear fractional boundary value problems are first linearized using the quasi-linearization technique, and then the ψ-Haar wavelet technique is applied to the linearized problem. The solution is updated by the ψ-Haar wavelet method in each iteration of the quasi-linearization technique. The proposed method is a good and simple mathematical technique for numerically solving non-linear ψ-FDEs. The operational matrix (OM) method is computationally more efficient. Several linear and non-linear boundary value problems are discussed to demonstrate the applicability, efficiency, and simplicity of the method. Moreover, the error analysis is carried out resulting a rigorous error bound for the proposed method.

4.1 Methodology for solution of ψ-fractional boundary value problem:

Consider the boundary value problem

$$ {}^{C}D_{\delta_1}^{\alpha,\psi} y(t) = g(t),\ 1 < \alpha \leq 2 \tag{4.1} $$

$$y(\delta_1) = y_{\delta_1} \quad y(\delta_2) = y_{\delta_2},$$

apply $\mathcal{I}_{\delta_1}^{\alpha,\psi}$ on equation (4.1)

$$\mathcal{I}_{\delta_1}^{\alpha,\psi\,C} D_{\delta_1}^{\alpha,\psi} y(t) = \mathcal{I}_{\delta_1}^{\alpha,\psi} g(t),$$

apply lemma 2.4.2 on L.H.S, we get

$$y(t) - c_0 - c_1\big(\psi(t) - \psi(\delta_1)\big) = \frac{1}{\Gamma(\alpha)} \int_{\delta_1}^{t} \big(\psi(t) - \psi(s)\big)^{\alpha-1} \psi'(s) g(s) ds. \tag{4.2}$$

Apply $y(\delta_1) = y_{\delta_1}$, equation (4.2) **implies $y_{\delta_1} = c_0$. Again apply $y(\delta_2) = y_{\delta_2}$ (put $t = \delta_2$ in equation** (4.2)**) we have,**

$$y_{\delta_2} - y_{\delta_1} - c_1\big(\psi(\delta_2) - \psi(\delta_1)\big) = \frac{1}{\Gamma(\alpha)} \int_{\delta_1}^{\delta_2} \big(\psi(\delta_2) - \psi(s)\big)^{\alpha-1} \psi'(s) g(s) ds.$$

$$\Rightarrow \quad c_1 = \frac{y_{\delta_1} - y_{\delta_2}}{\psi(\delta_2) - \psi(\delta_1)} + \frac{1}{\psi(s) - \psi(\delta_1)} \int_{\delta_1}^{\delta_2} \frac{(\psi(\delta_2) - \psi(s))}{\Gamma(\alpha)} \psi'(s) g(s) ds.$$

Substituting c_0 and c_1 in equation (4.2) **we obtained**

$$\begin{aligned} y(t) = y_{\delta_1} &+ \left[\frac{y_{\delta_1} - y_{\delta_2}}{\psi(\delta_2) - \psi(\delta_1)}\right] [\psi(t) - \psi(\delta_1)] \\ &+ \frac{\psi(t) - \psi(\delta_1)}{\psi(\delta_2) - \psi(\delta_1)} \int_{\delta_1}^{\delta_2} \frac{[\psi(\delta_2) - \psi(s)]^{\alpha-1}}{\Gamma(\alpha)} \psi'(s) g(s) ds \\ &+ \frac{1}{\Gamma(\alpha)} \int_{\delta_1}^{t} (\psi(t) - \psi(s))^{\alpha-1} \psi'(s) g(s) ds. \end{aligned}$$

The general case:
consider the boundary value problem

$$D_{\delta_1}^{\alpha,\psi} y(t) = g(t), t \in [\delta_1, \delta_2], \ n - 1 < \alpha \leq n, \tag{4.3}$$

with the initial and boundary conditions given by

$$y_{\psi}^{[\kappa]}(\delta_1) = y_{\delta_1}^{\kappa}, \ y_{\psi}^{[n-1]}(\delta_2) = y_{\delta_2}, \quad \kappa = 0, 1, 2, \cdots n - 2.$$

Apply $\mathcal{I}_{\delta_1}^{\alpha,\psi}$ on (4.3)

$$\mathcal{I}_{\delta_1}^{\alpha,\psi} \ {}^{C} D_{\delta_1}^{\alpha,\psi} y(t) = \mathcal{I}_{\delta_1}^{\alpha,\psi} g(t), \tag{4.4}$$

using Lemma 2.4.2 in equation (4.4)**, we have**

$$y(t) - \sum_{\kappa=0}^{n-1} \frac{y_{\psi}^{[\kappa]}(\delta_1)}{\kappa!} (\psi(t) - \psi(\delta_1))^{\kappa} = I^{\alpha,\psi} g(t)$$

$$y(t) = \sum_{\kappa=0}^{n-2} \frac{y_{\psi}^{[\kappa]}(\delta_1)}{\kappa!} (\psi(t) - \psi(\delta_1))^{\kappa} + \frac{y_{\psi}^{[n-1)}(\delta_1)}{(n-1)!} (\psi(t) - \psi(\delta_1))^{n-1} + \mathcal{I}_{\delta_1}^{\alpha,\psi} g(t)$$

$$y_{(t)} = \sum_{\kappa=0}^{n-2} \frac{y_{\delta_1}^{\kappa}}{\kappa!}(\psi(t) - \psi(\delta_1))^{\kappa} + C_{n-1}(\psi(t) - \psi(\delta_1))^{n-1} + \mathcal{I}_{\delta_1}^{\alpha,\psi} g(t) \tag{4.5}$$

where

$$C_{n-1} := \frac{y_{\psi}^{[n-1]}(\delta_1)}{(n-1)!}. \tag{4.6}$$

Now apply the boundary conditions

$$y_{\psi}^{(n-1)}(\delta_2) = y_{\delta_2} \tag{4.7}$$

we get

$$\begin{aligned}\left(\frac{1}{\psi'(t)}\frac{d}{dt}\right)^{n-1} y(t) = \sum_{\kappa=0}^{n-2} \frac{y_{\delta_1}^{\kappa}}{\kappa!} \left[\frac{1}{\psi'(t)}\frac{d}{dt}\right]^{n-1} (\psi(t) - \psi(\delta_1))^{\kappa} \\ + C_{n-1}\left[\frac{1}{\psi'(t)}\frac{d}{dt}\right]^{n-1} (\psi(t) - \psi(\delta_1))^{n-1} + \left[\frac{1}{\psi'(t)}\frac{d}{dt}\right]^{n-1} \mathcal{I}_{\delta_1}^{\alpha,\psi} g(t),\end{aligned} \tag{4.8}$$

where $\kappa = 0, 1, \cdots n-2$**.**

Note (1):

$$\frac{1}{\psi'(t)}\frac{d}{dt}(\psi(t) - \psi(\delta_1)) = \frac{1}{\psi'(t)}\psi'(t) = 1$$

and

$$\left(\frac{1}{\psi'(t)}\frac{d}{dt}\right)^{2} (\psi(t) - \psi(\delta_1))' = \frac{1}{\psi'(t)}\frac{d}{dt}(1) = 0.$$

In general

$$\left[\frac{1}{\psi'(t)}\frac{d}{dt}\right]^{n} (\psi(t) - \psi(\delta_1))^{m} = 0 \text{ **if** } m < n.$$

Note(2):

$$\frac{1}{\psi'(t)}\frac{d}{dt}(\psi(t) - \psi(\delta_1))^{n} = \frac{1}{\psi'(t)} n(\psi(t) - \psi(\delta_1))^{n-1}\psi'(t)$$

$$\left(\frac{1}{\psi'(t)}\frac{d}{dt}\right)^{2} (\psi(t) - \psi(\delta_1))^{n} = n(n-1)(\psi(t) - \psi(\delta_1))^{n-2}$$

$$\left(\frac{1}{\psi'(t)}\frac{d}{dt}\right)^{3} (\psi(t) - \psi(\delta_1))^{n} = n(n-1)(n-2)(\psi(t) - \psi(\delta_1))^{n-3}$$

$$\left(\frac{1}{\psi'(t)}\frac{d}{dt}\right)^m(\psi(t)-\psi(\delta_1))^n = n(n-1)(n-2)\cdots(n-m+1)(\psi(t)-\psi(\delta_1))^{n-m}$$
$$= \frac{n(n-1)(n-2)\cdots(n-m+1)(n-m)!}{(n-m)!}(\psi(t)-\psi(\delta_1))^{n-m}$$
$$= \frac{n!}{(n-m)!}[\psi(t)-\psi(\delta_1)]^{n-m},$$
if $m=n$, $\left[\frac{1}{\psi_1}\frac{d}{dt}\right]^n[\psi(t)-\psi(\delta_1)]^n = n!$.

Note (3):

$$\left[\mathcal{I}_{\delta_1}^{\alpha,\psi}h(t)\right]_{\psi}^{[\kappa]}(t) = \mathcal{I}_{\delta_1}^{\alpha-\kappa}h(t)$$

Or

$$\left[\frac{1}{\psi'(t)}\frac{d}{dt}\right]^{\kappa}\mathcal{I}_{\delta_1}^{\alpha,\psi}h(t) = \mathcal{I}_{\delta_1}^{\alpha-\kappa}h(t),$$

using note (1), (2), and (3) in equation (4.8)**, we have**

$$y_{\psi}^{(n-1)}(t) = (n-1)!C_{n-1} + \mathcal{I}_{\delta_1}^{\alpha-n+1}g(t),$$

apply the boundary conditions

$$y_{\psi}^{[n-1]}(\delta_2) = y_{\delta_2},$$

we have

$$C_{n-1} = \frac{1}{(n-1)!}\left[y_{\delta_2} - \mathcal{I}_{\delta_1}^{\alpha-n+1,\psi}g(\delta_2)\right].$$

Substituting C_{n-1} **in equation** (4.5)**, we get**

$$y_{(t)} = \sum_{\kappa=0}^{n-2}\frac{y_{\delta_1}^{\kappa}}{\kappa!}(\psi(t)-\psi(\delta_1))^{\kappa} + \frac{[\psi(t)-\psi(\delta_1)]^{n-1}}{(n-1)!}\left[y_{\delta_2} - \mathcal{I}_{\delta_1}^{\alpha-n+1,\psi}g(\delta_2)\right] + \mathcal{I}_{\delta_1}^{\alpha,\psi}g(t)$$

$$y_{(t)} = \sum_{\kappa=0}^{n-2}\frac{y_{\delta_1}^{\kappa}[\psi(t)-\psi(\alpha))}{\kappa!} + \frac{y_{\delta_2}}{(n-1)!}[\psi(t)-\psi(1))^{n-1}$$
$$- \frac{[\psi(t)-\psi(\delta_1)]^{n-1}}{(n-1)!}\int_{\delta_1}^{\delta_2}\frac{(\psi(\delta_2)-\psi(s)\psi'(s)}{\Gamma(\alpha-n+1)}g(s)ds + \int_{\delta_1}^{t}\frac{(\psi(t)-\psi(s))^{\alpha-1}}{\Gamma(\alpha)}\psi'(s)g(s)ds.$$

4.2 Numerical solutions of ψ-FDEs

Here are some numerical examples of how to approximate the numerical solution of the linear and non-linear boundary value problems of ψ-FDEs with our proposed method.

4.2.1 Linear Boundary Value Problems

Example 4.2.1. Consider the non-homogeneous fractional boundary value problem involving ψ-Caputo fractional derivative

$$\mathcal{D}_0^{\alpha,\psi} y(t) + ay(t) = g(t), \quad t \in [0,1],\ y(0) = 0,\ y(1) = y_1. \tag{4.9}$$

Where $1 < \alpha \leq 2$. For $g(t) = \psi(t) + a\frac{\psi(t)^{\alpha+1}}{\Gamma(\alpha+2)}$ and $y_1 = \frac{1}{\Gamma(\alpha+2)}$, the boundary value problem (3.1) has an exact solution $y(t) = \frac{(\psi(t))^{\alpha+1}}{\Gamma(\alpha+2)}$. The integral representation of (4.9) is given by

$$y(t) = -a\mathcal{I}_0^{\alpha,\psi} y(t) + a\psi(t)^{\alpha-1}\mathcal{I}_0^{\alpha,\psi} y(1) + h(t) \tag{4.10}$$

where

$$h(t) = \mathcal{I}_0^{\alpha,\psi} g(t) - \psi(t)^{\alpha-1}\mathcal{I}_0^{\alpha,\psi} g(1) + \frac{(\psi(t))^{\alpha-1}}{\Gamma(\alpha+2)}.$$

For numerical solution, we approximate $y(t)$ as

$$y(t) = C_m^T H_m(t). \tag{4.11}$$

Then

$$\mathcal{I}_0^{\alpha,\psi} y(t) = C_m^T \mathcal{I}_0^{\alpha,\psi} H_m(t) = C_m^T P_{m\times m}^{\alpha,\psi} H_m(t). \tag{4.12}$$

Let $\psi(t) = (\psi(t))^{\alpha-1}$, we have

$$\psi(t)\mathcal{I}_0^{\alpha,\psi} y(1) = C_m^T K_{m\times m}^{\alpha,\psi} H_m(t), \tag{4.13}$$

using equations (4.11), (4.12) and (4.13) in equation (4.9), to have:

$$C_m^T H_m(t) = -aC_m^T P_{m\times m}^{\alpha,\psi} H_m(t) + aC_m^T K_{m\times m}^{\alpha,\psi} H_m(t) + F_m^T H_m(t), \tag{4.14}$$

where $F_m^T H_m(t)$ is the approximation of $h(t)$.

In Figure 4.1, numerical solutions, exact solutions, and the max absolute-error are plotted for various choices of the function $\psi(t)$ and α. The max absolute-error is also shown in the Table 4.1 for various values of α and J. We discovered that as J increases, the max absolute-error also decreases.

Example 4.2.2. In this example we analyze the ψ-fractional differential equation with variable coefficients by the proposed method.

$$\mathcal{D}_0^{\alpha,\psi} y(t) + a(t)y(t) = h(t), \text{ where } 2 \leq \alpha < 3 \text{ and } t \in [0,1], \tag{4.15}$$

with the boundary conditions $y(0) = 0$, $y'(0) = 0$, $y(1) = 0$.

Table 4.1. max absolute-error for different J and α values.

		$\psi(t)=t$		
α	$J=5$	$J=6$	$J=7$	$J=8$
1.5	3.504635×10^{-5}	1.234185×10^{-5}	4.274255×10^{-6}	1.513357×10^{-6}
1.6	5.025384×10^{-5}	1.902764×10^{-5}	7.221228×10^{-5}	2.744912×10^{-5}
1.7	6.704913×10^{-5}	2.7187536×10^{-5}	1.103824×10^{-5}	4.482642×10^{-6}
1.8	7.817852×10^{-5}	3.393346×10^{-5}	1.474324×10^{-5}	6.404627×10^{-6}
1.9	6.675254×10^{-5}	3.148735×10^{-5}	1.458791×10^{-5}	6.812362×10^{-6}
		$\psi(t)=\frac{t^2}{2}+\frac{t}{2}$		
1.5	2.717725×10^{-5}	9.021482×10^{-6}	3.073846×10^{-6}	1.068451×10^{-6}
1.6	4.135072×10^{-5}	1.572354×10^{-5}	6.053439×10^{-6}	2.346431×10^{-6}
1.7	5.948473×10^{-5}	2.457804×10^{-5}	1.017341×10^{-5}	4.143252×10^{-6}
1.8	7.227815×10^{-5}	3.163172×10^{-5}	1.386834×10^{-5}	6.154427×10^{-6}
1.9	6.335346×10^{-5}	2.952634×10^{-5}	1.381907×10^{-5}	6.456180×10^{-6}

For numerical solution, we employ ψ-Haar wavelet method. Suppose

$$\mathcal{D}^{\alpha,\psi}y(t)=C_m^TH_m(t). \tag{4.16}$$

Using ψ-Caputo integral operator and the boundary conditions, we have

$$y(t)=C_m^TP_{m\times m}^{\alpha,\psi}H_m(t)-C_m^TK_{m\times m}^{\alpha,\psi}H_m(t). \tag{4.17}$$

Substituting equations (4.16) and (4.17) in equation (4.15), we get

$$C_m^T(H_m(t)+C_m^T\hat{P}_{m\times m}^{\alpha,\psi}(H_m(t)-C_m^TK_{m\times m}^{\alpha,\psi}H_m(t)=F_m^T(t)H_m(t), \tag{4.18}$$

where the following approximations are used

$$a(t)\mathcal{I}_0^{\alpha,\psi}H_m(t)=\hat{P}_{m\times m}^{\alpha,\psi}H_m(t),$$

$$\psi(t)\mathcal{I}_0^{\alpha,\psi}H_m(1)=K_{m\times m}^{\alpha,\psi}H_m(t)$$

$$h(t)=F_m^T(t)H_m(t)$$

where

$$\psi(t)=a(t)(\psi(t))^{\alpha-1}.$$

One may verify that for

$$a(t)=e^{-9\pi\psi(t)},\ h(t)=e^{-9\pi\psi(t)}\big((\psi(t))^{\alpha-1}-(\psi(t))^{\alpha}\big)-\Gamma(\alpha+1)$$

the boundary value problem (4.15) has the exact solution as $y(t)=\big(\frac{1}{\psi(t)}-1\big)(\psi(t))^{\alpha}$. For different choices of the function $\psi(t)$ and α, numerical solutions, exact solution and the maximum absolute error are plotted in the Figure 4.2. Also the maximum absolute error is presented in the Table 4.2 for various J and α.

Table 4.2. max absolute-error for $\psi(t) = t^3$ and different J and α values.

α	$J = 5$	$J = 6$	$J = 7$	$J = 8$
2.5	2.384237×10^{-5}	1.854308×10^{-5}	1.824315×10^{-5}	1.893752×10^{-5}
2.6	8.448743×10^{-6}	5.875834×10^{-6}	4.818904×10^{-6}	4.734526×10^{-6}
2.7	2.984073×10^{-6}	1.786233×10^{-6}	1.272453×10^{-6}	1.182537×10^{-6}
2.8	1.049082×10^{-6}	5.453306×10^{-7}	3.364195×10^{-7}	2.956827×10^{-7}

4.2.2 Non-linear Boundary value problems

Example 4.2.3. Consider the non-linear boundary value problem of fractional order with ψ-Caputo fractional derivative:

$$\mathcal{D}_0^{\alpha,\psi} y(t) + a(t)y'^2(t) + b(t)y(t)y'(t) = h(t), \text{ where } 1 < \alpha \leq 2, \text{and } t \in [0,1], \quad (4.19)$$

subject to boundary conditions $y(0) = 0,\ y(1) = 0$. The exact solution of equation (4.19) is given by $y(t) = (\psi(t))^\alpha - (\psi(t))^{70-\alpha}$. Where

$$\begin{aligned} h(t) = \Gamma(\alpha+1) - \frac{71-\alpha}{71-2\alpha}(\psi(t))^{70-2\alpha} + a(t)(\alpha(\psi(t))^{\alpha-1} - (70-\alpha)(\psi(t))^{69-\alpha})^2 \\ + b(t)(\alpha(\psi(t))^{\alpha-1} - (70-\alpha)(\psi(t))^{69-\alpha})((\psi(t))^\alpha - (\psi(t))^{70-\alpha}) \end{aligned}$$

We first linearize the non-linear terms in equation (4.19) by using quasi-linearization technique and then utilize ψ-Haar wavelet method for numerical solution.
Equation (4.19) in its linearized representation is given by:

$$\begin{aligned} &\mathcal{D}_0^{\alpha,\psi} y_{r+1}(t) + b(t)y'_r(t)y_{r+1}(t) + (2a(t)y'_r(t) + b(t)y_r(t))y'_{r+1}(t) \\ &= h(t) + a(t)y'^2_r(t) + b(t)y_r(t)y'_r(t),\ t > 0 \text{ and } 1 < \alpha \leq 2, \end{aligned} \quad (4.20)$$

having $y_{r+1}(0) = 0,\ y_{r+1}(1) = 0$ as the boundary conditions. The ψ-Haar wavelet approach is applied to equation (4.20). Let

$$\mathcal{D}_0^{\alpha,\psi} y_{r+1}(t) = C_m^T H_m(t). \quad (4.21)$$

Employing $\mathcal{I}^{\alpha,\psi}$ and the boundary conditions on (4.21), we have

$$y_{r+1}(t) = \mathcal{I}^{\alpha,\psi} C_m^T H_m(t) = C_m^T P_{m\times m}^{\alpha,\psi} H_m(t). \quad (4.22)$$

$$y'_{r+1}(t) = C_m^T P_{m\times m}^{\alpha-1,\psi} H_m(t). \quad (4.23)$$

Substituting (4.21), (4.22) and (4.23) in (4.20) we have,

$$\begin{aligned} &C_m^T\big(H_m(t) + b(t)y'_r(t)P_{m\times m}^{\alpha,\psi} H_m(t) + (2a(t)y'_r(t) + b(t)y_r(t))P_{m\times m}^{\alpha-1,\psi} H_m(t)\big) \\ &= h(t) + a(t)y'^2_r(t) + b(t)y_r(t)y'_r(t). \end{aligned} \quad (4.24)$$

In matrix notation, equation (4.24) can be written as:

$$C_m^T\big(H_m(t)+b(t)y_r'(t)P_{m\times m}^{\alpha,\psi}H_m(t)+(2a(t)y_r'(t) + b(t)y_r(t))P_{m\times m}^{\alpha-1,\psi}H_m(t)\big)=F(t), \tag{4.25}$$

where $F(t)=h(t)+a(t)y_r'^2(t)+b(t)y_r(t)y_r'(t)$.
The desired numerical solution is obtained by solving (4.25) for C_m^T and substituting the value of C_m^T in equation (4.23). Table 4.3 shows the max absolute-error for several J and α values. In Figure 4.3, the exact and approximate solutions for various selections of the function $\psi(t)$ are shown.

Table 4.3. Absolute error for various J and α values.

J	$\alpha=1.6$	$\alpha=1.7$	$\alpha=1.8$	$\alpha=1.9$	$\alpha=2.0$
5	1.981467×10^{-4}	1.637253×10^{-4}	1.253471×10^{-4}	9.497683×10^{-5}	7.13125×10^{-5}
6	6.389746×10^{-5}	4.824637×10^{-5}	3.526588×10^{-5}	2.516453×10^{-5}	1.753205×10^{-5}
7	2.0568703×10^{-5}	1.435892×10^{-5}	9.874581×10^{-6}	6.624682×10^{-6}	4.413058×10^{-6}
8	6.6420531×10^{-6}	4.346458×10^{-6}	2.785478×10^{-6}	1.753052×10^{-6}	1.105386×10^{-6}

Example 4.2.4. Consider the fractional order non-linear Lane Emden boundary value problem with ψ-Caputo fractional derivative

$$\mathcal{D}_0^{\alpha,\psi}y(t)+\frac{2}{\psi(t)}y'(t)-6y^2(t)=h(t), \tag{4.26}$$

where $1<\alpha\leq 2,$ and $t\in[0,1]$. Subject to the boundary conditions

$$y(0)=0, \quad y(1)=2.$$

For $\alpha=2$ and $h(t)=6+\frac{2}{\psi(t)}-6((\psi(t))^2+\psi(t))^2$, the exact solution of the problem (4.26) is given by $y(t)=(\psi(t))^2+\psi(t)$.
We first linearize the non-linear terms in equation (4.26) using the Quasilinearization technique, and then use the ψ-Haar wavelet approach to determine the numerical solution of the linearized FDE using the same procedure as in example 4.2.3.
The max absolute-error for various α and J values is shown in Table 4.4. In Figure 4.4, the exact and approximate solutions for various selections of α and their max absolute-error are plotted.

4.3 Conclusion

Operational matrices approach has been applied for the fist time to ψ-FDEs with boundary conditions. One of the major advantages of the technique is

Table 4.4. max absolute error for $\psi(t) = \tan(\frac{t}{2})$ and different choices of α, J.

		$\zeta = 0.5$ and $\alpha = 0.75$		
α	$J = 5$	$J = 6$	$J = 7$	$J = 8$
1.5	6.405136×10^{-6}	2.372232×10^{-6}	8.34561×10^{-7}	2.450634×10^{-7}
1.6	3.866363×10^{-6}	1.233445×10^{-6}	3.756732×10^{-7}	1.234257×10^{-7}
1.7	3.213574×10^{-6}	8.766463×10^{-7}	2.391531×10^{-7}	5.643642×10^{-8}
1.8	2.827468×10^{-6}	7.563442×10^{-7}	1.746525×10^{-7}	4.686534×10^{-8}
1.9	2.457272×10^{-6}	5.846783×10^{-7}	1.584563×10^{-7}	3.532453×10^{-8}

that it is a convenient and effective numerical scheme for solution of non-linear ψ-FDEs. The operational matrices are sparse matrices, which help to reduce the computational cost of the method. The numerical scheme given in this study is based on ψ-Haar wavelet OMs of integration. For linear and non-linear ψ-FDEs, these OMs are generated and successfully used to solve two and multi-point boundary value problems. Other wavelet bases, such as Gegenbauer, Chebyshev, and Legendre wavelet, can be used with the proposed technique. The proposed method can be used to solve ψ-fractional partial differential equations as well.

Approximate solutions of equation (3.1) for different choices of $\psi(t)$ and α.

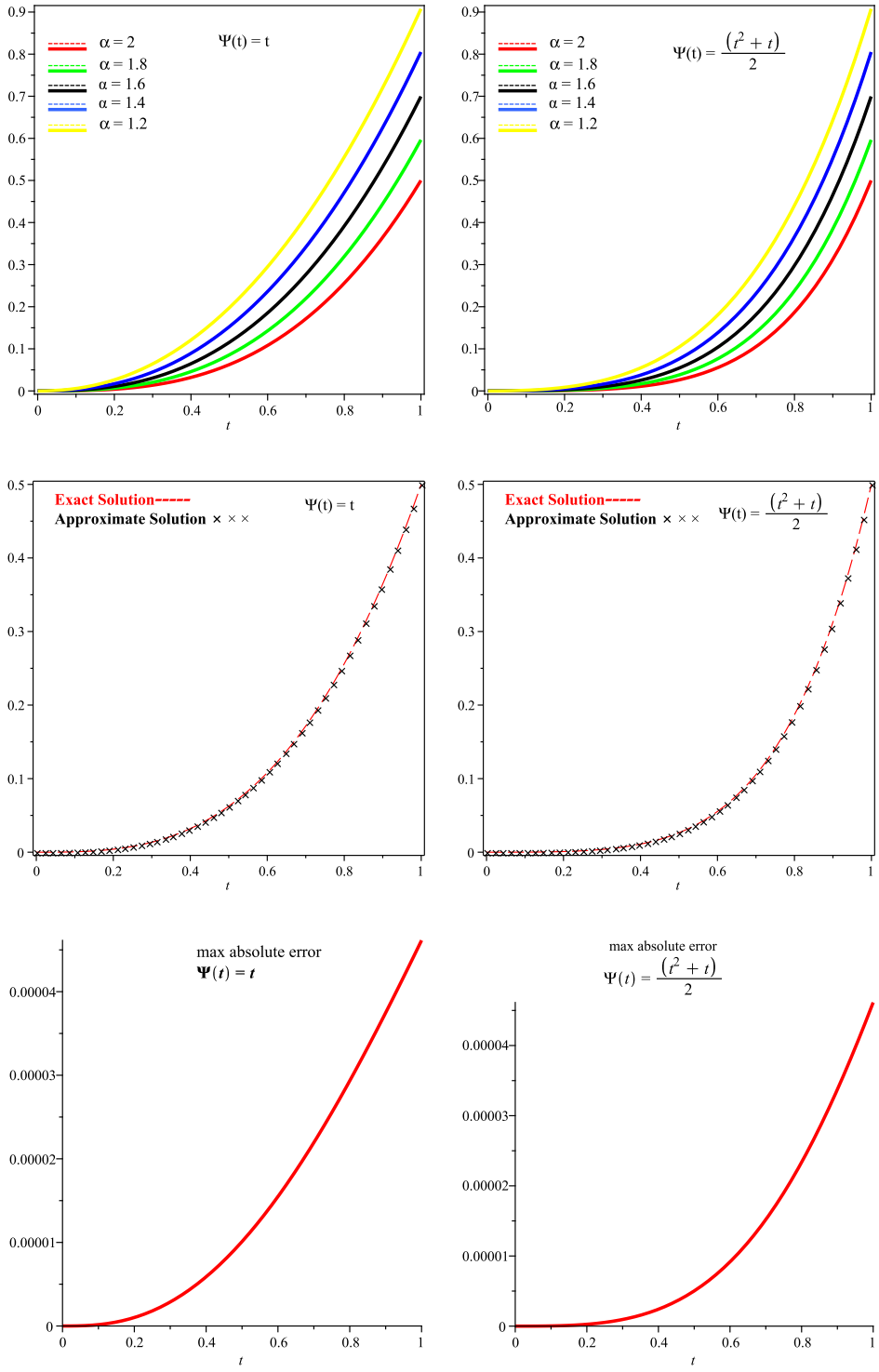

Figure 4.1: Exact and Approximate solutions and the corresponding max absolute error of equation (3.1) for $\psi(t) = t$ and $\psi(t) = (t^2 + t)/2$.

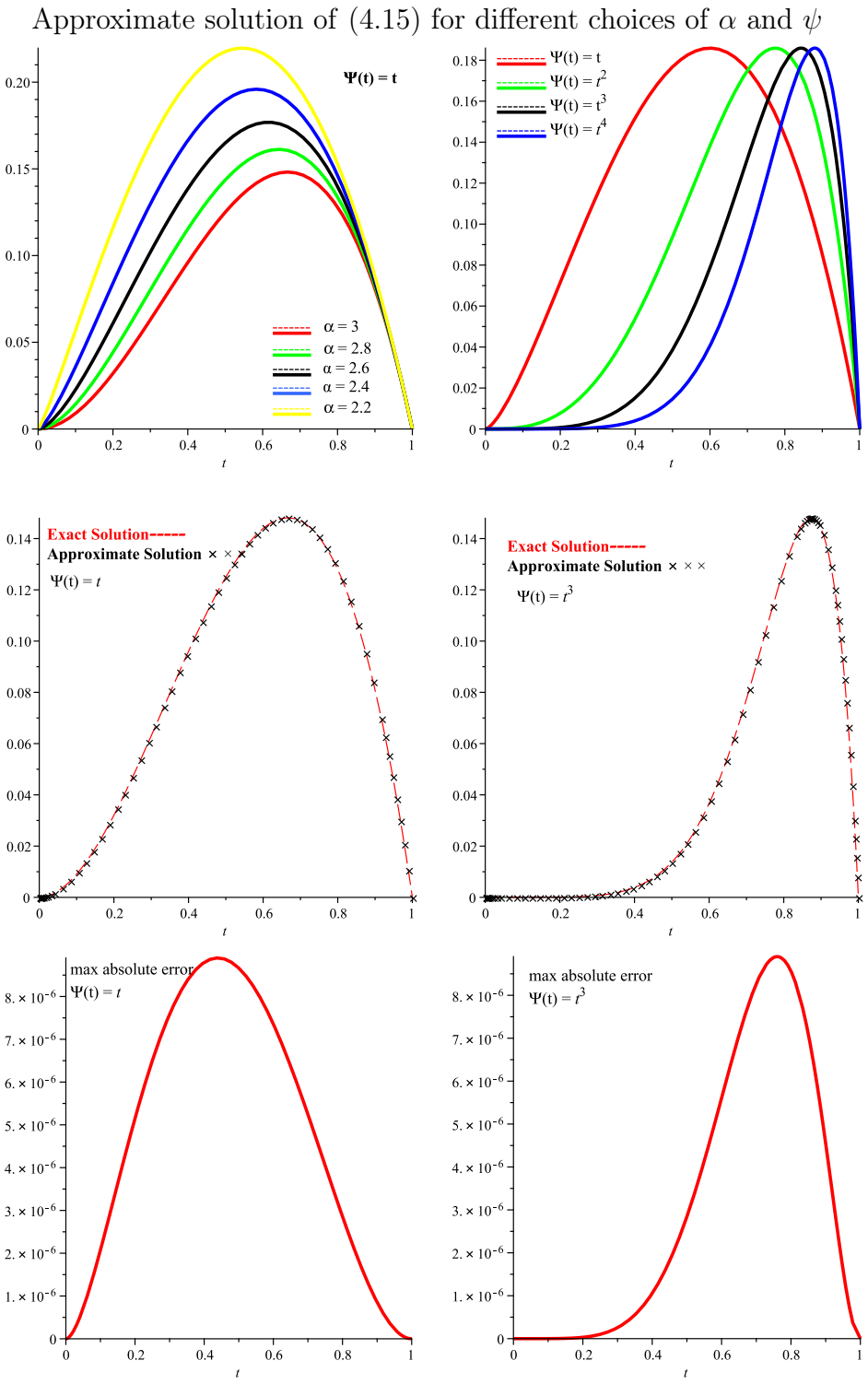

Figure 4.2: For equation (4.15). Exact and approximate solutions for $\psi(t) = t$ and $\psi(t) = t^3$ and the corresponding max absolute error.

For equation (4.19):Exact and Approximate solutions for different choices of ψ

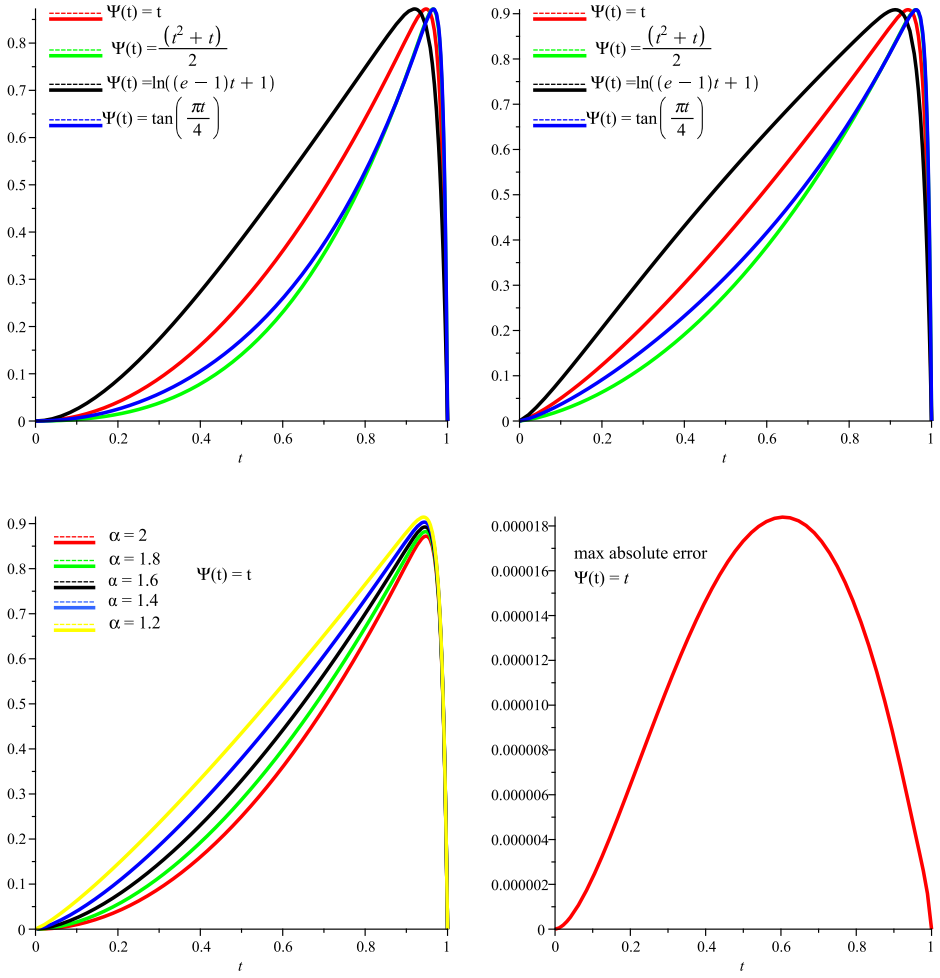

Figure 4.3: For equation (4.19):Approximate solutions for different choices of α and the max absolute error.

Numerical solutions of (4.26) for $\psi(t) = t$ and $\psi(t) = \tan(\frac{t}{2})$ for different values of α

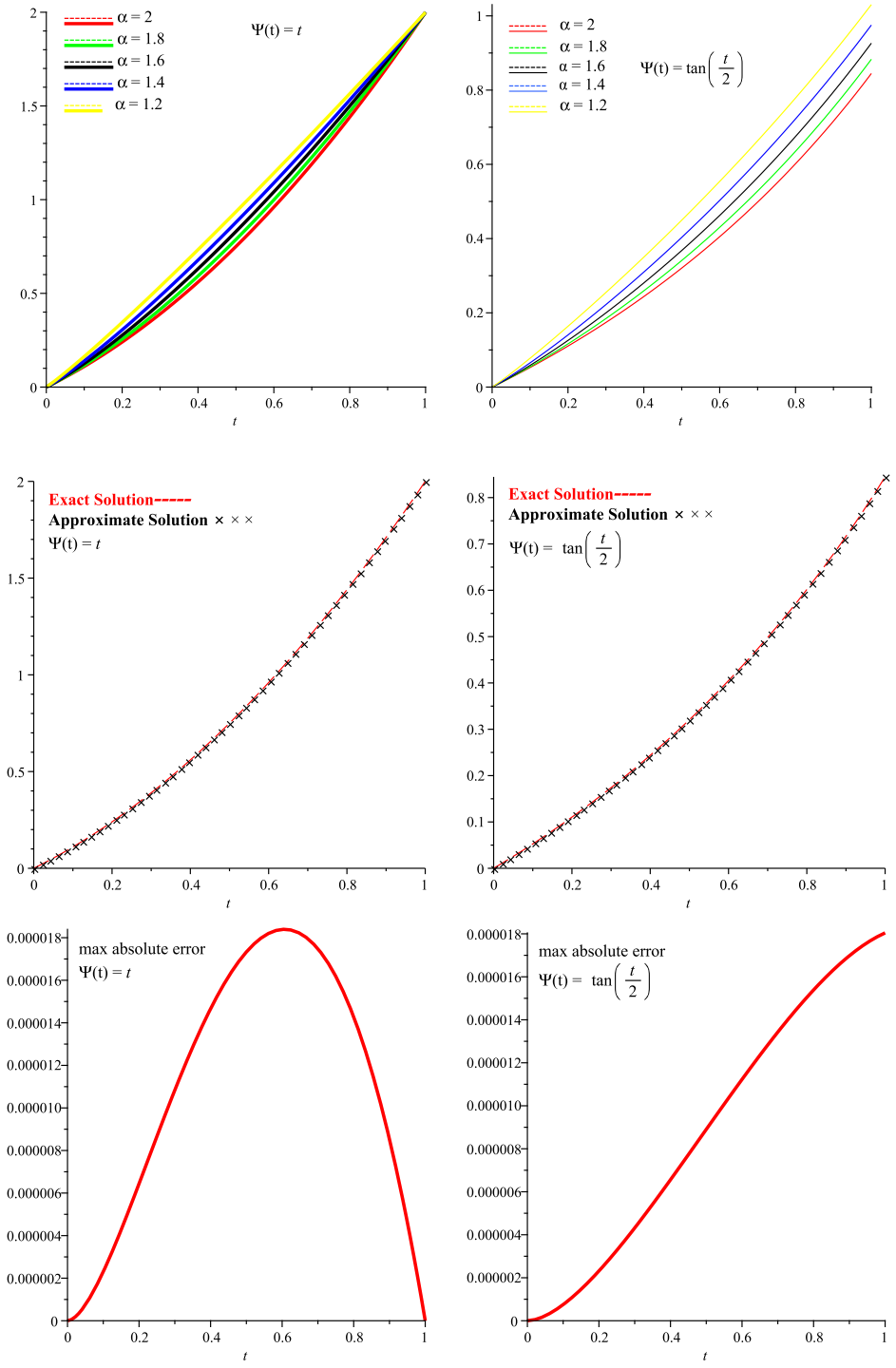

Figure 4.4: exact and approximate solutions of (4.26) for $\psi(t) = t$ and $\psi(t) = \tan(\frac{t}{2})$ and the corresponding max absolute error.

Chapter 5

Numerical Solution to ψ-Fractional Partial Differential Equations (ψ-FPDEs)

In this chapter we extended the ψ-Haar wavelet methods for boundary value problems to develop a technique for numerical solutions of linear ψ-FPDEs. This technique is based on our paper [60]

5.1 ψ-FPDEs with constant coefficients

In this section we discuss numerical solutions of linear FPDEs with constant coefficients involving ψ-Caputo fractional derivative.

$$\frac{\partial^{\alpha,\psi} y(x,t)}{\partial t^{\alpha,\psi}} + \lambda \frac{\partial^{\beta,\psi} y(x,t)}{\partial t^{\beta,\psi}} + \mu y(x,t) = \eta \frac{\partial^{\gamma,\psi} y(x,t)}{\partial x^{\gamma,\psi}} + f(x,t), \tag{5.1}$$

where $0 < \alpha \leq 2$, $0 \leq \beta \leq 1$, and $1 \leq \gamma \leq 2$, and have non-homogeneous boundary and initial conditions given by

$$y(x,0) = \rho(x), \ \frac{\partial y(x,t)}{\partial t}|_{t=0} = \sigma(x), \ y(0,t) = \xi(t), \ y(1,t) = \zeta(t). \tag{5.2}$$

For $1 < \alpha \leq 2$ and λ, μ, $\eta > 0$, the equation (5.1) reduces to the fractional telegraph equation. For special cases, it includes the heat, wave, and Poisson equations. The ψ-Haar wavelets technique provides numerical solutions. By approximating $\frac{\partial^{\alpha,\psi} y(x,t)}{\partial t^{\alpha,\psi}}$ using two-dimensional Haar wavelets, we have:

$$\frac{\partial^{\alpha,\psi} y(x,t)}{\partial t^{\alpha,\psi}} = H_m^T(x) C_{m\times m} H_m(t). \tag{5.3}$$

Operating both sides of equation (5.3) **by** $\mathcal{I}_t^{\alpha,\psi}$**, we get:**

$$y(x,t) = H_m^T(x)C_{m\times m}\Big(\int_0^t \psi'(t)\frac{(\psi(t)-\psi(s))^{\alpha-1}}{\Gamma(\alpha)}H_m(s)ds\Big) + p(x)t + q(x). \tag{5.4}$$

Applying the initial conditions $y(x,0) = \rho(x)$, $\frac{\partial y(x,t)}{\partial t}|_{t=0} = \sigma(x)$**, from equation** (5.2) **we have** $q(x) = \rho(x)$ **and** $p(x) = \sigma(x)$**. Therefore equation** (5.4) **becomes**

$$y(x,t) = H_m^T(x)C_{m\times m}P_{m\times m}^{\alpha,\psi}H_m(t) + \sigma(x)t + \rho(x). \tag{5.5}$$

Applying $\frac{\partial^{\beta,\psi}}{\partial t^{\beta,\psi}}$ **to equation** (5.5)**, we obtain**

$$\frac{\partial^{\beta,\psi}y(x,t)}{\partial t^{\beta,\psi}} = H_m^T(x)C_{m\times m}P_{m\times m}^{\alpha-\beta,\psi}H_m(t) + \sigma(x)\frac{t^{1-\beta}}{\Gamma(2-\beta)}. \tag{5.6}$$

By substituting equations (5.3)**,** (5.5) **and** (5.6) **in equation** (5.1)**, we have**

$$\begin{aligned}\eta\frac{\partial^{\gamma,\psi}y(x,t)}{\partial x^{\gamma,\psi}} &= H_m^T(x)C_{m\times m}H_m(t) + \lambda H_m^T(x)C_{m\times m}P_{m\times m}^{\alpha-\beta,\psi}H_m(t)\\ &\quad +\mu H_m^T(x)C_{m\times m}P_{m\times m}^{\alpha,\psi}H_m(t) + g(x,t)\\ &= H_m^T(x)\bigg(C_{m\times m}(I+\lambda P_{m\times m}^{\alpha-\beta,\psi}+\mu P_{m\times m}^{\alpha,\psi}+G_{m\times m})\bigg)H_m(t),\end{aligned} \tag{5.7}$$

where

$$g(x,t) = \sigma(x)\left(\frac{\lambda t^{1-\beta}}{\Gamma(2-\beta)}+\mu t\right) + \mu\rho(x) - f(x,t) = H_m^T(x)G_{m\times m}H_m(t).$$

Applying $\mathcal{I}_x^{\gamma,\psi}$ **on both sides of equation** (5.7)**, we have**

$$\begin{aligned}\eta y(x,t) = \mathcal{I}_x^{\gamma,\psi}H_m^T(x)&\bigg(C_{m\times m}(I+\lambda P_{m\times m}^{\alpha-\beta,\psi}+\mu P_{m\times m}^{\alpha,\psi}+G_{m\times m})\bigg)H_m(t)\\ &+x\phi_1(t)+\phi_2.\end{aligned} \tag{5.8}$$

Implementing the conditions $y(0,t) = \xi(t)$**,we get** $\phi_2(t) = \xi(t)$ **and** $y(1,t) = \zeta(t)$ **gives**

$$\begin{aligned}\phi_1(t) = \mathcal{I}_x^{\gamma,\psi}H_m^T(1)&\bigg(C_{m\times m}(I+\lambda P_{m\times m}^{\alpha-\beta,\psi}+\mu P_{m\times m}^{\alpha,\psi}+G_{m\times m})\bigg)H_m(t)\\ &+\zeta(t)-\xi(t).\end{aligned} \tag{5.9}$$

Substituting equation (5.9) **in equation** (5.8) **we have**

$$\begin{aligned}\eta y(x,t) &= H_m^T(x)\Big((P_{m\times m}^{\gamma,\psi})^T - (Q_{m\times m}^{\gamma,\psi})^T\Big)\\ &\times\Big\{C_{m\times m}(I+\lambda P_{m\times m}^{\alpha-\beta,\psi}+\mu P_{m\times m}^{\alpha,\psi}+G_{m\times m})\Big\}H_m(t)+x(\zeta(t)-\xi(t))+\xi(t).\end{aligned} \tag{5.10}$$

where

$$\mathcal{I}_x^{\gamma,\psi}H_m(x) = P_{m\times m}^{\gamma,\psi}H_m(x) = H_m^T(x)(P_{m\times m}^{\gamma,\psi})^T$$

and

$$x\mathcal{I}_x^{\gamma,\psi}H_m(1) = Q_{m\times m}^{\gamma,\psi}H_m(x).$$

From equation (5.5) **and equation** (5.10) **we get the Sylvester equation**

$$\begin{aligned}&\Big((P_{m\times m}^{\gamma,\psi})^T - (Q_{m\times m}^{\gamma,\psi})^T\Big)\Big(C_{m\times m}(I+\lambda P_{m\times m}^{\alpha-\beta,\psi}+\mu P_{m\times m}^{\alpha,\psi}\Big) - \eta C_{m\times m}P_{m\times m}^{\alpha,\psi}\\ &= S_{m\times m} - \Big((P_{m\times m}^{\gamma,\psi})^T - (Q_{m\times m}^{\gamma,\psi})^T\Big)G_{m\times m},\end{aligned} \tag{5.11}$$

where $s(x,t) = x(\zeta(t)-\xi(t))+\xi(t)-\eta(\sigma(x)t+\varrho(t)) = H_m^T(x)S_{m\times m}H_m(t)$**. Solving equation** (5.11) **for** $C_{m\times m}$ **and using equation** (5.5) **or equation** (5.6) **we can get the solution of the problem** (5.1)

5.2 ψ-FPDEs with variable coefficients

This section discusses the procedure for numerical solutions of the following class of ψ**-FPDEs.**

$$\frac{\partial^{\gamma,\psi}y(x,t)}{\partial t^{\gamma,\psi}} - a(x)\frac{\partial^{\alpha,\psi}y(x,t)}{\partial x^{\alpha,\psi}} + b(x)\frac{\partial^{\beta,\psi}y(x,t)}{\partial x^{\beta,\psi}} + d(x)y(x,t) = f(x,t), \tag{5.12}$$

where $1<\alpha\leq 2$**,** $1<\beta\leq 2$**,** $0<\gamma\leq 2$ **and with the initial conditions:**

$$y(x,0)=\phi_1(x),\ \frac{y(x,t)}{\partial t}\ |_{t=0}=\psi_1(x),\ \textbf{or}\ y(x,0)=\phi_1(x),\ y(x,1)=\psi_2(x) \tag{5.13}$$

and boundary conditions:

$$y(0,t)=\mu(t),\ y(1,t)=\nu(t), \tag{5.14}$$

Here, we present a numerical technique based on ψ**-Haar wavelets operational matrices for** ψ**-fractional integration. We approximate** $\frac{\partial^{\alpha,\psi}y(x,t)}{\partial x^{\alpha,\psi}}$ **with Haar wavelets as**

$$\frac{\partial^{\alpha,\psi}y(x,t)}{\partial x^{\alpha,\psi}} = H_m^T(x)C_{m\times m}H_m(t). \tag{5.15}$$

Operating $\mathcal{I}_x^{\alpha,\psi}$ on equation (5.15), we get

$$y(x,t) = \mathcal{I}_x^{\alpha,\psi} H_m^T(x) C_{m\times m} H_m(t) + p(t)x + q(t). \tag{5.16}$$

Applying boundary conditions in equation (5.14), to equation (5.16), we have

$$q(t) = \mu(t), \quad p(t) = -\mathcal{I}_x^{\alpha,\psi} H_m^T(x) C_{m\times m} H_m(t) + \nu(t) - \mu(t). \tag{5.17}$$

Therefore, equation (5.16) can be written as

$$\begin{aligned} y(x,t) =& \mathcal{I}_x^{\alpha,\psi} H_m^T(x) C_{m\times m} H_m(t) - x\mathcal{I}_x^{\alpha,\psi} H_m^T(x) C_{m\times m} H_m(t) \\ &+ x(nu(t) - \mu(t)) + \mu(t). \end{aligned} \tag{5.18}$$

Since $\mathcal{I}_x^{\alpha,\psi} H_m(x) = P_{m\times m}^{\alpha,\psi} H_m(x)$ and $\phi^1(x)\mathcal{I}_x^{\alpha,\psi} H_m(x) = Q_{m\times m}^{\alpha,1}$, where $\phi^1(x) = x$. Therefore (5.18) takes the form

$$\begin{aligned} y(x,t) =& H_m^T(x)(P_{m\times m}^{\alpha,\psi})^T C_{m\times m} H_m(t) - H_m^T(x)(Q_{m\times m}^{\alpha,1})^T C_{m\times m} H_m(t) \\ &+ x(\nu(t) - \mu(t)) + \mu(t). \end{aligned} \tag{5.19}$$

Applying the ψ-Caputo operator $\frac{\partial^{\beta,\psi}}{\partial x^\beta}$ on (5.18), we have

$$\begin{aligned} \frac{\partial^{\beta,\psi} y(x,t)}{\partial x^\beta} =& \mathcal{I}_x^{\alpha,\psi} H_m^T(x) C_{m\times m} H_m(t) - \frac{x^{1-\beta}}{\Gamma(2-\beta)} \mathcal{I}_x^{\alpha,\psi} H_m^T(x) C_{m\times m} H_m(t) \\ &+ \frac{x^{1-\beta}}{\Gamma(2-\beta)}(nu(t) - \mu(t)) + \mu(t). \end{aligned} \tag{5.20}$$

For simplicity, we introduced some convenient notations.

$$\begin{aligned} &\phi_2 = \frac{b(x)x^{1-\beta}}{\Gamma(2-\beta)}, \\ &\phi_3 = xd(x), \\ &r(x,t) = \frac{x^{1-\beta}}{\Gamma(2-\beta)}(nu(t) - \mu(t)) + d(x)q(t) + (\nu(t) - \mu(t))xd(x), \\ &s(x,t) = x(\nu(t) - \mu(t)) + \mu(t) + \psi_1(x)t + \phi_1(x), \\ &g(x,t) = x(\nu(t) - \mu(t)) - \mu(t) + (\psi_2(x) - \phi_1(x))t + \phi_1(x) \\ &d(x)\mathcal{I}_x^{\alpha,\psi} H_m(x) = \bar{P}_{m\times m}^{\alpha,\psi} H_m(x), \quad b(x)\mathcal{I}_x^{\alpha,\psi} H_m(x) = \bar{P}_{m\times m}^{\alpha,\psi} H_m(x). \end{aligned}$$

Substituting equations (5.15)**,** (5.18)**, and** (5.20) **in equation** (5.12)**, we have**

$$\begin{aligned} \frac{\partial^{\gamma,\psi} y(x,t)}{\partial t^{\gamma,\psi}} = \Bigg(& a(x)H_m^T(x) - H_m^T(x)(\bar{P}_{m\times m}^{\alpha-\beta})^T + H_m^T(x)(Q_{m\times m}^{2,\alpha})^T - H_m^T(x)(\bar{P}_{m\times m}^{\alpha})^T \\ &+ H_m^T(x)(Q_{m\times m}^{\alpha,3})^T \Bigg) C_{m\times m} H_m(t) + H_m^T(x) R_{m\times m} H_m(t). \end{aligned}$$

Applying $\mathcal{I}_x^{\gamma,\psi}$ on previous equation, we get

$$y(x,t) = \Bigg(a(x)H_m^T(x) - H_m^T(x)(P_{m\times m}^{\alpha-\beta})^T + H_m^T(x)(Q_{m\times m}^{2,\alpha})^T - H_m^T(x)(\bar{P}_{m\times m}^{\alpha})^T + H_m^T(x)(Q_{m\times m}^{\alpha,3})^T \Bigg) C_{m\times m}\mathcal{I}_x^{\gamma,\psi}H_m(t) + H_m^T(x)R_{m\times m}\mathcal{I}_x^{\gamma,\psi}H_m(t) + w(x)t + \omega(x).$$

Using the initial conditions, we get $\omega(x) = \phi_1(x)$ and $w(x) = \psi_1(x)$. Therefore

$$y(x,t) = \Bigg(a(x)H_m^T(x) - H_m^T(x)(\bar{P}_{m\times m}^{\alpha-\beta})^T + H_m^T(x)(Q_{m\times m}^{2,\alpha})^T - H_m^T(x)(\bar{P}_{m\times m}^{\alpha})^T + H_m^T(x)(Q_{m\times m}^{\alpha,3})^T \Bigg) C_{m\times m}\mathcal{I}_x^{\gamma,\psi}H_m(t) + H_m^T(x)R_{m\times m}\mathcal{I}_x^{\gamma,\psi}H_m(t) + \psi_1(x)t + \phi_1(x). \tag{5.21}$$

Now, we employ the boundary conditions to get $w(x) = \phi_1(x)$ and

$$\begin{aligned} v(x) = \Bigg[\Bigg(& a(x)H_m^T x - H_m^T x(\hat{P}_{m\times m}^{\alpha-\beta,\psi})^T + H_m^T x(Q_{m\times m}^{\alpha,\psi,2})^T - H_m^T x(\bar{P}_{m\times m}^{\alpha,\psi})^T \\ & + H_m^T x(Q_{m\times m}^{\alpha,\psi,3})^T \Bigg) C_{m\times m} + H_m^T x R_{m\times m} \Bigg] \mathcal{I}_t^{\gamma} H_m(1) + \psi_2 x - \phi_1(x). \end{aligned} \tag{5.22}$$

Therefore, equation (5.21) becomes

$$\begin{aligned} y(x,t) = \Bigg[\Bigg(& a(x)\psi_M^T(x) - H_m^T(x)(\hat{P}_{m\times m}^{\alpha-\beta,\psi})^T + H_m^T(x)(Q_{m\times m}^{\alpha,\psi,2})^T - H_m^T(x)(\bar{P}_{m\times m}^{\alpha,\psi})^T \\ & + H_m^T(x)(Q_{m\times m}^{\alpha,\psi,3})^T \Bigg) C_{m\times m} + H_m^T(x)R_{m\times m} \Bigg] \big(P_{m\times m}^{\gamma} - Q_{m\times m}^{\gamma}\big)\psi_m(t) \\ & + (\psi_2(x) - \phi(x))t + \phi_1(x). \end{aligned} \tag{5.23}$$

Combining equations (5.19) and (5.21) gives the Sylvester equation

$$\begin{aligned} \Bigg((P_{m\times m}^{\alpha,\psi})^T - (Q_{m\times m}^{\alpha,\psi,1})^T \Bigg) C_{m\times m} - \Bigg(& \frac{\eta}{m}\psi_{m\times m}A_{m\times m}H_{m\times m}^T - (\hat{P}_{m\times m}^{\alpha-\beta,\psi}) - (\bar{P}_{m\times m}^{\alpha,\psi})^T \\ & + (Q_{m\times m}^{\alpha,\psi,2})^T + (Q_{m\times m}^{\alpha,\psi,3})^T \Bigg) C_{m\times m}P_{m\times m}^{\gamma} = R_{m\times m}P_{m\times m}^{\gamma} + S_{m\times m}, \end{aligned} \tag{5.24}$$

where $A_{m\times m} := diag[(a(x_i))]$, $x_i = \frac{2i-1}{2m}$, $i = 1, 2, 3, \cdots, m$. Also, using equations (5.19) **and** (5.23)**, we obtain the following matrix form:**

$$\begin{aligned}\Big((P^{\alpha,\psi}_{m\times m})^T - (Q^{\alpha,\psi,1}_{m\times m})^T\Big)C_{m\times m} - \Big(\frac{\eta}{m}\psi_{m\times m}A_{m\times m}H^T_{m\times m} - (\hat{P}^{\alpha-\beta,\psi}_{m\times m})\\ - (\bar{P}^{\alpha,\psi}_{m\times m})^T + (Q^{\alpha,\psi,2}_{m\times m})^T + (Q^{\alpha,\psi,3}_{m\times m})^T\Big) \times C_{m\times m}\big(P^{\gamma}_{m\times m} - Q^{\gamma}_{m\times m}\big)\\ = R_{m\times m}\big(P^{\gamma}_{m\times m} - Q^{\gamma}_{m\times m}\big) + G_{m\times m}.\end{aligned} \tag{5.25}$$

By solving equation (5.25) **for** $G_{m\times m}$ **and substituting it into equation** (5.19)**, we get the approximate solution of problem** (5.12)**.**
To solve various ψ-FPDEs, we use the ψ-Haar wavelets technique. Additionally, we compared the graphical results obtained using the proposed method with the exact solutions. For the first two examples we use the technique discussed in the subsection 5.1 and for the other two examples we follow the procedure discussed in subsection 5.2

Example 5.2.1. For example one, consider the time-fractional telegraph equation with ψ-Caputo fractional derivative

$$\begin{aligned}&\frac{\partial^{\alpha,\psi}y(x,t)}{\partial t^{\alpha,\psi}} + \frac{\partial^{\alpha-1,\psi}y(x,t)}{\partial t^{\alpha-1,\psi}} + y(x,t) = \frac{\partial^2 y(x,t)}{\partial x^2}\\ &+ \frac{\Gamma(2\alpha+1)}{\Gamma(\alpha+1)}\Big(1+\frac{\psi(t)}{\alpha+1}\Big)(\psi(t))^{\alpha,\psi}\cos(7x) + 50(\psi(t))^{2\alpha}\cos(7x),\end{aligned} \tag{5.26}$$

satisfying the initial and boundary conditions

$$y(x,0) = 0, \frac{\partial y(x,t)}{\partial t}|_{t=0} = 0, y(0,t) = (\psi(t))^{2\alpha}, y(1,t) = 0.7539022(\psi(t))^{2\alpha}.$$

The exact solution for the problem (5.26) is given by: $y(x,t) = (\psi(t))^{2\alpha}\cos(7x)$. Exact and approximate solutions of the problem (5.26) and their absolute error are plotted in Figure 5.1. Also absolute error for problem (5.26) is given in Table 5.1 for various choices of the parameters $\alpha,\ J,\ t$ and x.

Example 5.2.2. Consider the ψ-FPDE given by:

$$\begin{aligned}\frac{\partial^{\alpha,\psi}y(x,t)}{\partial t^{\alpha,\psi}} - \lambda\frac{\partial^2 y(x,t)}{\partial x^2} = \Big(\frac{(\psi(t))^{1-\alpha}}{\Gamma(2-\alpha)} - \frac{\Gamma(3\alpha+1)}{\Gamma(2\alpha+1)}(\psi(t))^{2\alpha}\Big)\\ + 144\lambda\psi(t)(1-(\psi(t))^{3\alpha-1})\sin(12x),\end{aligned} \tag{5.27}$$

where $0 \le \alpha \le 1$, and with the initial and boundary conditions:

$$y(x,0) = y(0,t) = 0, y(1,t) = -0.536573\psi(t)(1-(\psi(t))^{3\alpha-1}).$$

Table 5.1. Absolute error for $\psi(x) = \sin(x)$

t	x	α	$J = 3$	$J = 4$	$J = 5$	$J = 6$	$J = 7$
0.25	0.20	1.5	3.3780×10^{-3}	7.4702×10^{-4}	2.4498×10^{-5}	8.0425×10^{-6}	2.6428×10^{-6}
	0.50	1.6	2.1513×10^{-3}	6.5313×10^{-4}	1.9862×10^{-5}	6.0507×10^{-6}	1.8462×10^{-6}
	0.80	1.7	2.0818×10^{-3}	5.8754×10^{-4}	1.6603×10^{-5}	4.6985×10^{-6}	1.3317×10^{-6}
0.50	0.20	1.8	2.0718×10^{-3}	5.4730×10^{-4}	1.4458×10^{-5}	3.8213×10^{-6}	1.0106×10^{-6}
	0.50	1.9	2.0363×10^{-3}	5.3432×10^{-4}	1.3359×10^{-5}	3.3400×10^{-6}	8.3502×10^{-7}
	0.80	2.0	2.0363×10^{-4}	5.3432×10^{-4}	1.3359×10^{-5}	3.3400×10^{-6}	8.3502×10^{-7}

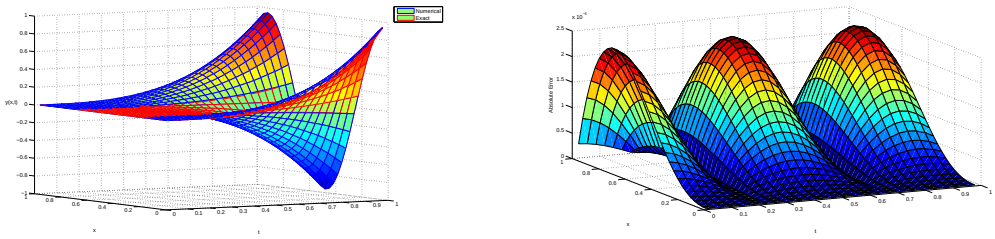

Figure 5.1: Approximate and exact solutions of equation (5.26) and their absolute error.

The exact solution of problem (5.27) is given by

$$y(x,t) = \sin(12x)\psi(t)(1 - (\psi(t))^{3\alpha-1}).$$

Approximate and exact solution of the problem (5.27) and their absolute error are plotted in Figure 5.2.

Also the maximum absolute error is presented in the Table 5.2.

Table 5.2. Maximum absolute error for $\psi(x) = x^2$ and different values of J and α.

t	x	α	$J = 3$	$J = 4$	$J = 5$	$J = 6$	$J = 7$
0.25	0.20	0.5	4.3007×10^{-2}	4.1167×10^{-4}	4.5672×10^{-5}	3.2361×10^{-5}	3.4349×10^{-6}
	0.50	0.6	6.3553×10^{-3}	6.2332×10^{-4}	5.4130×10^{-5}	4.2321×10^{-6}	2.6340×10^{-7}
	0.80	0.7	4.6571×10^{-3}	2.7212×10^{-5}	4.2014×10^{-6}	3.1478×10^{-6}	4.3216×10^{-7}
0.50	0.20	0.8	6.5786×10^{-4}	6.7634×10^{-5}	6.3132×10^{-6}	4.7324×10^{-7}	3.6210×10^{-7}
	0.50	0.9	2.1714×10^{-4}	5.3452×10^{-6}	3.0884×10^{-6}	4.2703×10^{-7}	5.7381×10^{-8}
	0.80	1.0	3.2738×10^{-5}	1.2753×10^{-6}	2.8801×10^{-7}	4.6721×10^{-8}	8.5382×10^{-9}

Example 5.2.3. Consider the linear fractional diffusion equation with ψ-Caputo derivative

$$\frac{\partial y(x,t)}{\partial t} = a(x)\frac{\partial^{1.8,\psi} y(x,t)}{\partial x^{1.8,\psi}} + f(x,t), \tag{5.28}$$

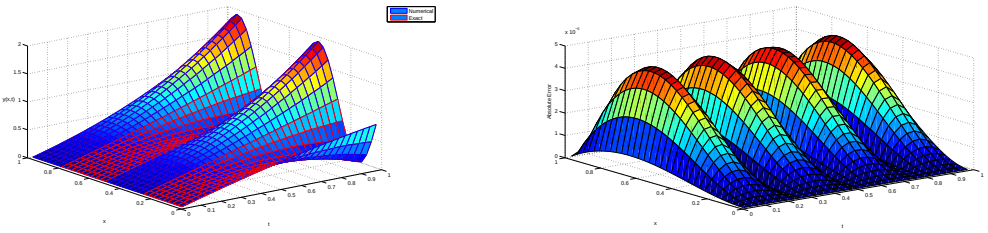

Figure 5.2: Approximate and exact solutions of equation (5.27) and their absolute error.

with initial and boundary conditions $y(x,0) = (\psi(x))^2(1-\psi(x))$ and $(0,t) = 0, y(1,t) = 0$ respectively.

For $a(x) = \Gamma(1.2)(\psi(x))^{1.8}$ and $f(x,t) = (6\psi(x)-3)(\psi(x))^2e^{-t}$, the problem (5.28) has the exact solution $y(x,t) = ((\psi(x))^2 - (\psi(x))^3)e^{-t}$. Numerical and exact solutions using ψ-Haar wavelets technique and their absolute error for $\alpha = 1.8$ and $J = 5$ are shown in Figure 5.3.

Table 5.3. Absolute error for $t = 0.25$, $t = 0.5$, different values of J, α and $\psi(x) = x^3$

t	x	α	$J=3$	$J=4$	$J=5$	$J=6$	$J=7$
0.25	0.20	1.5	1.2733×10^{-3}	6.2471×10^{-4}	3.0934×10^{-4}	1.5391×10^{-4}	7.6766×10^{-5}
	0.50	1.6	1.2910×10^{-3}	6.3216×10^{-4}	3.1273×10^{-4}	1.5552×10^{-4}	7.7551×10^{-5}
	0.80	1.7	1.1161×10^{-3}	5.4369×10^{-4}	2.6824×10^{-4}	1.3321×10^{-4}	6.6382×10^{-5}
0.50	0.20	1.8	7.1349×10^{-4}	3.4173×10^{-4}	1.6710×10^{-4}	8.2612×10^{-5}	4.1071×10^{-5}
	0.50	2.0	6.1030×10^{-5}	1.5258×10^{-5}	3.8146×10^{-6}	9.5367×10^{-7}	2.3841×10^{-7}

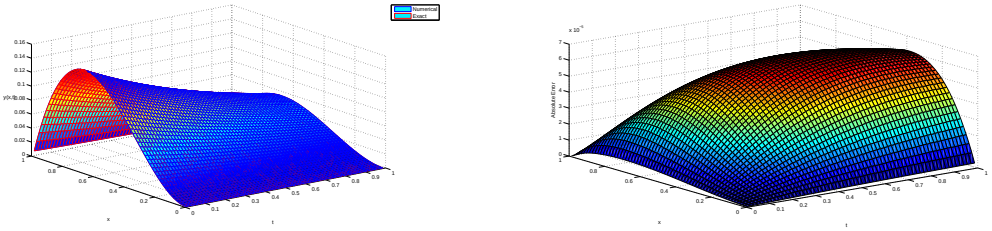

Figure 5.3: Approximate and exact solutions of equation (5.28) and their absolute error.

Example 5.2.4. Here we consider the convection-diffusion equation with ψ-Caputo fractional derivative:

$$\frac{\partial^{\gamma,\psi} y(x,t)}{\partial t^{\gamma,\psi}} = -ax\frac{\partial^{\alpha,\psi} y(x,t)}{\partial x^{\alpha,\psi}} + bx\frac{\partial^{\beta,\psi} y(x,t)}{\partial x^{\beta,\psi}} + f(x,t), \tag{5.29}$$

where $1 < \alpha \leq 2$, $0 < \beta \leq 1$, $0 < \gamma \leq 2$ and with initial and boundary conditions: $y(x,0) = y(x,1) = 0$ $y(0,t) = 0$, $y(1,t) = 0$. We solve this problem with $a(x) = \Gamma(\beta+2)\Gamma(5-\{\alpha+\beta\})\psi(x)^{\beta}$, $b(x) = \Gamma(2\beta+2-\alpha)\Gamma(5-2\alpha)\psi(x)^{\alpha}$, and

$$\begin{aligned} f(x,t) =& (2\pi\psi(x)^{2\beta+1} - \psi(x)^{4-\alpha})\psi(t)^{1-\gamma}E_{2,2-\gamma}(-(2\pi\psi(t))^2) \\ &+ \Big(\Gamma(2\beta+2)\Gamma(5-\{\alpha+\beta\}) - \Gamma(5-2\alpha)\psi(x)^{2\beta+1} \\ &+ \Gamma(5-2\alpha)(\Gamma(2\beta+2-\alpha) - \Gamma(\beta+2))\psi(x)^{4-\alpha}\Big)\sin(2\pi\psi(t)). \end{aligned}$$

The exact solution of the problem (5.29) is

$$y(x,t) = (\psi(x)^{2\beta+1} - \psi(x)^{4-\alpha})\sin(2\pi\psi(t)).$$

Exact and approximate solutions of problem 5.29 and their absolute error is plotted in Figure 5.4. Also absolute error is given in Table 5.4. for various values of α, x and J at $t = 0.25$ and $t = 0.50$.

Table 5.4. Absolute error for $\psi(x) = x^2$

t	x	α	$J=3$	$J=4$	$J=5$	$J=6$	$J=7$
0.25	0.20	1.5	4.3854×10^{-4}	1.4252×10^{-4}	4.6203×10^{-5}	1.4996×10^{-5}	4.8789×10^{-6}
	0.50	1.6	3.3031×10^{-4}	1.0001×10^{-4}	3.0183×10^{-5}	9.1122×10^{-6}	2.7562×10^{-6}
	0.80	1.7	2.4252×10^{-4}	6.8593×10^{-5}	1.9314×10^{-5}	5.4339×10^{-6}	1.5301×10^{-6}
0.50	0.20	1.8	1.7673×10^{-4}	4.6930×10^{-5}	1.2396×10^{-5}	3.2674×10^{-6}	8.6081×10^{-7}
	0.50	2.0	1.3575×10^{-4}	3.4133×10^{-5}	8.5580×10^{-6}	2.1426×10^{-6}	5.3605×10^{-7}

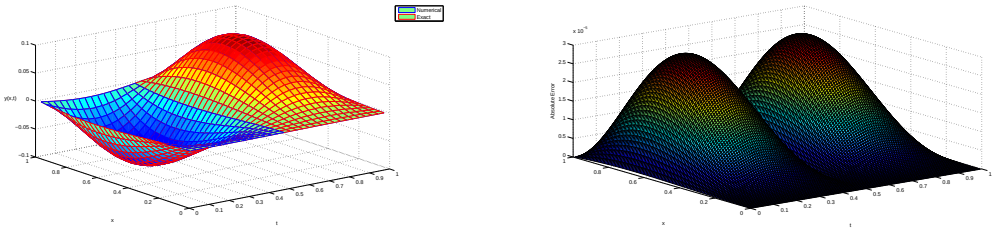

Figure 5.4: Approximate and exact solutions of equation (5.29) and their absolute error.

5.3 Conclusion

We developed and used the ψ-Haar wavelets operational matrix of integration of fractional order for the first time for numerical solution of ψ-FPDEs.

The numerical results of the proposed method are compared to the exact solutions and illustrated along with their absolute error in the figures. Furthermore, the absolute errors are presented in tables, indicating that our method agrees well with the exact solutions. The proposed method can also be applied to other wavelet bases, such as Legendre, Chebyshev, and Gegenbauer wavelets and can also be applied to nonlinear ψ-FPDEs.

Chapter 6

Conclusion

Fractional differential equations are the best way to model many real-world physical phenomena. Apart from modelling, solution strategies and their repercussions are essential for determining critical points where a significant divergence or bifurcation begins. As a result, high-precision solutions are always required.The ψ-Caputo fractional derivatives give additional flexibility to mathematical models, and the ψ-Caputo derivative has the ability to extract hidden features of real-world phenomena. We have derived the ψ-Haar wavelet operational matrix of fractional order integration. This matrix is successfully utilized to solve linear and nonlinear fractional differential equations involving ψ-Caputo fractional derivative with initial and boundary conditions. This method is simple and more convergent comparatively to the other methods. We solved several linear and nonlinear initial and boundary value problems using ψ-Haar wavelet operational matrix method. We also extended this method to solve fractional partial differential equations involving ψ-Caputo fractional derivative with initial and boundary conditions. Furthermore, we also performed error analysis from which we found error bound. ψ-Haar wavelets technique can also be extended to solve ψ-fractional nonlinear partial differential equations. The method may be extended to other wavelet basis, including Legendre wavelets, Chebyshev wavelets, and Gegenbauer wavelets.

Bibliography

[1] R. Almeida, "A caputo fractional derivative of a function with respect to another function," *Communications in Nonlinear Science and Numerical Simulation*, vol. 44, pp. 460–481, 2017.

[2] J. C. Domingues, "Sf lacroix, traité du calcul différentiel et du calcul intégral, (1797–1800)," in *Landmark Writings in Western Mathematics 1640-1940*, pp. 277–291, Elsevier, 2005.

[3] J. Liouville, *Mémoire sur quelques questions de géométrie et de mécanique, et sur un nouveau genre de calcul pour résoudre ces questions.* 1832.

[4] L. Debnath and W. J. Grum, "The fractional calculus and its role in the synthesis of special functions: Part i," *International Journal of Mathematical Education in Science and Technology*, vol. 19, no. 2, pp. 215–230, 1988.

[5] G. H. Hardy and J. E. Littlewood, "Some properties of fractional integrals. i.," *Mathematische Zeitschrift*, vol. 27, no. 1, pp. 565–606, 1928.

[6] A. Kilbas, *Theory and applications of fractional differential equations.*

[7] K. Oldham and J. Spanier, *The fractional calculus theory and applications of differentiation and integration to arbitrary order.* Elsevier, 1974.

[8] I. Podlubny, "Fractional differential equations, 198 academic press," *San Diego, California, USA*, 1999.

[9] A. A. Kilbas, O. Marichev, and S. Samko, "Fractional integrals and derivatives (theory and applications)," 1993.

[10] K. Diethelm, *The Analysis of Fractional Differential Equations: An Application-Oriented Exposition Using Differential Operators of Caputo Type.* Springer Science & Business Media, 2010.

[11] T. J. Osler, "The fractional derivative of a composite function," *SIAM Journal on Mathematical Analysis*, vol. 1, no. 2, pp. 288–293, 1970.

[12] J. Vanterler da C Sousa and E. Capelas de Oliveira, "On the ψ-fractional integral and applications," *Computational and Applied Mathematics*, vol. 38, no. 1, pp. 1–22, 2019.

[13] R. Almeida, "Fractional differential equations with mixed boundary conditions," *Bulletin of the Malaysian Mathematical Sciences Society*, vol. 42, no. 4, pp. 1687–1697, 2019.

[14] R. Almeida, A. B. Malinowska, and T. Odzijewicz, "On systems of fractional differential equations with the ψ-caputo derivative and their applications," *Mathematical Methods in the Applied Sciences*, vol. 44, no. 10, pp. 8026–8041, 2021.

[15] R. Almeida, A. B. Malinowska, and M. T. T. Monteiro, "Fractional differential equations with a caputo derivative with respect to a kernel function and their applications," *Mathematical Methods in the Applied Sciences*, vol. 41, no. 1, pp. 336–352, 2018.

[16] R. Almeida, M. Jleli, and B. Samet, "A numerical study of fractional relaxation–oscillation equations involving ψ-caputo fractional derivative," *Revista de la Real Academia de Ciencias Exactas, Físicas y Naturales. Serie A. Matemáticas*, vol. 113, no. 3, pp. 1873–1891, 2019.

[17] D. Sierociuk, A. Dzieliński, G. Sarwas, I. Petras, I. Podlubny, and T. Skovranek, "Modelling heat transfer in heterogeneous media using fractional calculus," *Philosophical Transactions of the Royal Society A: Mathematical, Physical and Engineering Sciences*, vol. 371, no. 1990, p. 20120146, 2013.

[18] V. V. Kulish and J. L. Lage, "Application of fractional calculus to fluid mechanics," *J. Fluids Eng.*, vol. 124, no. 3, pp. 803–806, 2002.

[19] C. Lederman, J.-M. Roquejoffre, and N. Wolanski, "Mathematical justification of a nonlinear integro-differential equation for the propagation of spherical flames," *Annali di Matematica Pura ed Applicata*, vol. 183, no. 2, pp. 173–239, 2004.

[20] R. L. Magin, "Fractional calculus models of complex dynamics in biological tissues," *Computers & Mathematics with Applications*, vol. 59, no. 5, pp. 1586–1593, 2010.

[21] N. Engheta, "On fractional calculus and fractional multipoles in electromagnetism," *IEEE Transactions on Antennas and Propagation*, vol. 44, no. 4, pp. 554–566, 1996.

[22] F. Mainardi, "Fractional calculus," in *Fractals and fractional calculus in continuum mechanics*, pp. 291–348, Springer, 1997.

[23] M. M. Meerschaert and C. Tadjeran, "Finite difference approximations for two-sided space-fractional partial differential equations," *Applied numerical mathematics*, vol. 56, no. 1, pp. 80–90, 2006.

[24] A. Arikoglu and I. Ozkol, "Solution of fractional differential equations by using differential transform method," *Chaos, Solitons & Fractals*, vol. 34, no. 5, pp. 1473–1481, 2007.

[25] S. El-Wakil, A. Elhanbaly, and M. Abdou, "Adomian decomposition method for solving fractional nonlinear differential equations," *Applied Mathematics and Computation*, vol. 182, no. 1, pp. 313–324, 2006.

[26] I. Hashim, O. Abdulaziz, and S. Momani, "Homotopy analysis method for fractional ivps," *Communications in Nonlinear Science and Numerical Simulation*, vol. 14, no. 3, pp. 674–684, 2009.

[27] I. Aziz *et al.*, "New algorithms for the numerical solution of nonlinear fredholm and volterra integral equations using haar wavelets," *Journal of Computational and Applied Mathematics*, vol. 239, pp. 333–345, 2013.

[28] M. Dehghan and M. Lakestani, "Numerical solution of nonlinear system of second-order boundary value problems using cubic b-spline scaling functions," *International Journal of Computer Mathematics*, vol. 85, no. 9, pp. 1455–1461, 2008.

[29] W. Dahmen, A. Kurdila, and P. Oswald, *Multiscale wavelet methods for partial differential equations*. Elsevier, 1997.

[30] V. Comincioli, G. Naldi, and T. Scapolla, "A wavelet-based method for numerical solution of nonlinear evolution equations," *Applied numerical mathematics*, vol. 33, no. 1-4, pp. 291–297, 2000.

[31] J.-L. Wu, "A wavelet operational method for solving fractional partial differential equations numerically," *Applied mathematics and computation*, vol. 214, no. 1, pp. 31–40, 2009.

[32] L. A. Díaz, M. T. Martín, and V. Vampa, "Daubechies wavelet beam and plate finite elements," *Finite Elements in Analysis and Design*, vol. 45, no. 3, pp. 200–209, 2009.

[33] X. Zhu, G. Lei, and G. Pan, "On application of fast and adaptive periodic battle–lemarie wavelets to modeling of multiple lossy transmission lines," *Journal of Computational physics*, vol. 132, no. 2, pp. 299–311, 1997.

[34] E. Babolian and F. Fattahzadeh, "Numerical solution of differential equations by using chebyshev wavelet operational matrix of integration," *Applied Mathematics and computation*, vol. 188, no. 1, pp. 417–426, 2007.

[35] U. Saeed, M. ur Rehman, and M. A. Iqbal, "Modified chebyshev wavelet methods for fractional delay-type equations," *Applied Mathematics and Computation*, vol. 264, pp. 431–442, 2015.

[36] Ö. Oruç, A. Esen, and F. Bulut, "A unified finite difference chebyshev wavelet method for numerically solving time fractional burgers' equation," *Discrete & Continuous Dynamical Systems-S*, vol. 12, no. 3, p. 533, 2019.

[37] Ü. Lepik, "Numerical solution of evolution equations by the haar wavelet method," *Applied Mathematics and Computation*, vol. 185, no. 1, pp. 695–704, 2007.

[38] C. Chen and C. Hsiao, "Haar wavelet method for solving lumped and distributed-parameter systems," *IEE Proceedings-Control Theory and Applications*, vol. 144, no. 1, pp. 87–94, 1997.

[39] F. BULUT, Ö. ORUC, and A. Esen, "Numerical solutions of fractional system of partial differential equations by haar wavelets," *CMES-Computer Modeling in Engineering & Sciences*, vol. 108, no. 4, 2015.

[40] Ö. Oruç, A. Esen, and F. Bulut, "A haar wavelet approximation for two-dimensional time fractional reaction–subdiffusion equation," *Engineering with Computers*, vol. 35, no. 1, pp. 75–86, 2019.

[41] A. Esen, F. Bulut, and Ö. Oruç, "A unified approach for the numerical solution of time fractional burgersâĂŹ type equations," *The European Physical Journal Plus*, vol. 131, no. 4, pp. 1–13, 2016.

[42] M. ur Rehman and R. A. Khan, "The legendre wavelet method for solving fractional differential equations," *Communications in Nonlinear Science and Numerical Simulation*, vol. 16, no. 11, pp. 4163–4173, 2011.

[43] U. Saeed, "Sine–cosine wavelets operational matrix method for fractional nonlinear differential equation," *International Journal of Wavelets, Multiresolution and Information Processing*, vol. 17, no. 04, p. 1950026, 2019.

[44] U. Saeed *et al.*, "Hermite wavelet method for fractional delay differential equations," *Journal of Difference Equations*, vol. 2014, 2014.

[45] G. M. Mittag-Leffler, "Sur la nouvelle fonction eα (x)," *CR Acad. Sci. Paris*, vol. 137, no. 2, pp. 554–558, 1903.

[46] A. Wiman, "Über den fundamentalsatz in der teorie der funktionen ea (x)," *Acta Mathematica*, vol. 29, pp. 191–201, 1905.

[47] A. Shukla and J. Prajapati, "On a generalization of mittag-leffler function and its properties," *Journal of mathematical analysis and applications*, vol. 336, no. 2, pp. 797–811, 2007.

[48] R. E. Bellman and R. Kalaba, *Quasilinearization and Nonlinear Boundary-Value Problems*. American Elsevier Publishing Co., Inc., New York, 1965.

[49] S. D. Conte and C. De Boor, *Elementary numerical analysis: an algorithmic approach*. SIAM, 2017.

[50] R. Almeida, A. B. Malinowska, and T. Odzijewicz, "An extension of the fractional gronwall inequality," in *Conference on Non-Integer Order Calculus and Its Applications*, pp. 20–28, Springer, 2018.

[51] Y. Li and W. Zhao, "Haar wavelet operational matrix of fractional order integration and its applications in solving the fractional order differential equations," *Applied mathematics and computation*, vol. 216, no. 8, pp. 2276–2285, 2010.

[52] Ü. Lepik and E. Tamme, "Solution of nonlinear fredholm integral equations via the haar wavelet method.," in *Proceedings of the Estonian Academy of Sciences, Physics, Mathematics*, vol. 56, 2007.

[53] K. Maleknejad and F. Mirzaee, "Using rationalized haar wavelet for solving linear integral equations," *Applied Mathematics and Computation*, vol. 160, no. 2, pp. 579–587, 2005.

[54] Y. Chen, M. Yi, and C. Yu, "Error analysis for numerical solution of fractional differential equation by haar wavelets method," *Journal of Computational Science*, vol. 3, no. 5, pp. 367–373, 2012.

[55] E. Babolian and A. Shahsavaran, "Numerical solution of nonlinear fredholm integral equations of the second kind using haar wavelets," *Journal of Computational and Applied Mathematics*, vol. 225, no. 1, pp. 87–95, 2009.

[56] A. Ali, T. Minamoto, U. Saeed, and M. U. Rehman, "ψ-haar wavelets method for numerically solving fractional differential equations," *Engineering Computations*, vol. 38, no. 2, pp. 1037–1056, 2021.

[57] U. Saeed and M. ur Rehman, "Haar wavelet–quasilinearization technique for fractional nonlinear differential equations," *Applied Mathematics and Computation*, vol. 220, pp. 630–648, 2013.

[58] P. Sunthrayuth, N. H. Aljahdaly, A. Ali, R. Shah, I. Mahariq, and A. M. Tchalla, "ϕ-haar wavelet operational matrix method for fractional relaxation-oscillation equations containing ϕ-caputo fractional derivative," *Journal of function spaces*, vol. 2021, pp. 1–14, 2021.

[59] A. Ali and T. Minamoto, "A new numerical technique for investigating boundary value problems with ψ-caputo fractional operator," *Journal of Applied Analysis & Computation*, vol. 13, no. 1, pp. 275–297, 2023.

[60] A. Ali, T. Minamoto, R. Shah, and K. Nonlaopon, "A novel numerical method for solution of fractional partial differential equations involving the ψ-caputo fractional derivative," *AIMS Mathematics*, vol. 8, no. 1, pp. 2137–2153, 2023.